

Computational and Matrix Isolation Infrared Spectroscopic Studies of Hydroxypyridyl and Pyridyloxy Radicals

Divanshu Gupta

MS14013

**A dissertation submitted for the partial fulfilment
of BS-MS dual degree in Science**



Indian Institute of Science Education and Research Mohali

April 2019

To,

My Family

"Live a Life Less Ordinary"

CERTIFICATE OF EXAMINATION

This is to certify that the dissertation titled “**Computational and Matrix Isolation Infrared Spectroscopic Studies of Hydroxypyridyl and Pyridyloxy Radicals**” submitted by Mr. Divanshu Gupta (Registration Number: MS14013) for the partial fulfilment of BS-MS dual degree programme of Indian Institute of Science Education and Research, Mohali has been examined by the thesis committee duly appointed by the institute. The committee finds the work done by the candidate satisfactory and recommends that the report be accepted.

Dr. Sugumar Venkataramani

(Supervisor)

Prof. K. S. Viswanathan

(Committee member)

Dr. P. Balanarayan

(Committee member)

Dated:

DECLARATION

The work presented in this dissertation has been carried out by me under the guidance of Dr. Sugumar Venkataramani at the Indian Institute of Science Education and Research, Mohali. This work has not been submitted in part or in full for a degree, a diploma, or a fellowship to any university or institute. Whenever contributions of others are involved, every effort is made to indicate this clearly, with due acknowledgement of collaborative research and discussion. This thesis is a bonafide record of original work done by me and all sources listed within have been detailed in the bibliography.

Divanshu Gupta

(Candidate)

Dated:

In my capacity as the supervisor of the candidate's project work, I certify that the above statements by the candidate are true to the best of my knowledge.

Dr. Sugumar Venkataramani

(Supervisor)

ACKNOWLEDGEMENTS

First and foremost, many thanks go to Dr. Sugumar Venkataramani, my supervisor, who believed in me, my qualities, and set off on an adventure of a lifetime with a smile! Thinking about getting the opportunity to work with him, I cannot help but wonder at my extremely fantastic luck! At times of grave desperation, it was his constant motivation, contagious enthusiasm and relentless passion for science that dragged me out of the dark and placed right on track again. While he gave me complete independence regarding the execution of my research work which helped to build my scientific mind to a great extent, I never found his office door shut for a quick discussion or a long pending trouble-shooting. I sincerely thank him for all his efforts, in developing and shaping me as a student, a presenter, and a human being, above all.

I want to thank Prof. K.S. Viswanathan and Dr. P. Balanarayan, the members of my thesis committee, for their invaluable and timely suggestions and unconditional mentorships. Thank you for your support and advice that set the stage for my dissertation work.

I am grateful to Prof. N. Sathyamurthy and Prof. Debi Prasad Sarkar, former Directors, IISER Mohali, for providing me the opportunity to work in this esteemed institute. I would also like to extend my gratitude towards Prof. Arvind, Director IISER Mohali, for giving me an opportunity to use the excellent infrastructures available in this premier research institute for smooth execution of my experimental works.

My honest thanks to IISER Mohali, and Department of Chemical Sciences, for giving me a chance to work in this wonderful environment. I am thankful to IISER Mohali for providing me with excellent facilities and faculties who helped in shaping my understanding of science to a great extent. I thank all of my teachers at IISER Mohali, who trained me in various fields of chemistry, and helped to build a scientific attitude and often taught me how to approach a scientific problem, which I am sure would remain indispensable in my future endeavors.

Further, I would like to thank my POC family including Chitranjan Shah, Mayank Saraswat, Anjali Mahadevan, Virinder Bhagat, Amandeep Singh, Himanshu Kumar, Ankit Gaur, Debpriya, Anjali Srivastva, Surbhi Grewal, Pravesh Kumar, Amal Sam Sunny, J Vaitheesh, and Irin P. Tom.

My special thanks to Chitranjan Shah for mentoring and guiding me right from the beginning like an elder brother, and for his valuable suggestions, support and off course for entertaining me

throughout the year and finally to Anjali Mahadevan and Mayank Saraswat for his very helping and caring nature at every point of time that I spent in lab.

Although graduate students definitely form the core of any lab in this part of the world, no lab can deny its debt to the undergrads. I have been fortunate enough to work with a number of exceptionally bright and hard-working undergraduate students. This dissertation work would not have been feasible for me to carry out without the unconditional and unquestioning help I received from my lab mates.

It will be right-out lying if I say that my voyage of MS never faced a bottomless pit. This would have definitely felt deeper, had I not been fortunate enough to have met people like Ruchika, Dagar, Sanjay, Promit, Soumitra, Manoj, Panda, Devra, Panda (not sure if I am missing out anybody) and many other residents of the four great hostels of IISER Mohali. I am sure they not only enlightened me about the various other important (or unimportant) things happening in the outer world other than science but also must have played a significant role in prolonging my sufferings through their constant motivation, encouragement and carefree celebration of the exuberance of life! Without this amazing group of people, I can see neither me nor this dissertation reaching their current state of existences.

I also thank Gupta Ji, for all those extra cups of tea, which often proved to be an elixir!

In addition to that, I am highly grateful to my family for believing me at every point of my life and for providing me their ever-ending support. My special thanks to my elder brothers, Uttam and Ashish for their continuous support.

I bow to the Mountains for keeping me alive!

At last (but whether it is least is up to the reader), I thank the elegant and elusive kingdom of Nature which has woven an intricate piece of art-work around it where its very existence is balanced upon its knowledge about itself and for allowing us to be bemused in its infinite and marvelous spectacles.

CONTENTS

ACKNOWLEDGEMENTS	
LIST OF ABBREVIATIONS	i
LIST OF FIGURES	iii
LIST OF TABLES	v
LIST OF SCHEMES	vii
Abstract	ix
Chapter 1. Introduction	1-4
1.1 Introduction to Free Radical Chemistry	
1.2 Heterocyclic Radicals	
1.3 Phenoxy Radicals	
1.4 Motivation and Scope of the Current Work	
1.5 Approaches	
Chapter 2. Results and Discussion	5-35
2.1 System of Interest	
2.2 Geometrical Parameters	
2.3 Stability Order of Monoradicals	
2.4 Bond Dissociation Energy (BDE)	
2.5 Spin Density	
2.6 Electrostatic Potential (ESP)	
2.7 Natural Bond Orbital (NBO) Analysis	
2.8 Nuclear Independent Chemical Shift (NICS)	
2.9 Reactivity	
2.9.1 1,2-H Shift	
2.9.2 1,3-H Shift	

2.10 Biradicals	
2.10.1 Singlet-Triplet Energy Gap of Biradicals	
2.10.2 Second BDE	
2.11 Matrix Isolation	
2.11.1 Deposition of 2-iodo-3-hydroxypyridine	
2.11.2 Formation of 2-Dehydro-3-hydroxypyridine Radical	
2.11.3 Formation of ketene and carbene	
2.11.4 Formation of other photoproducts	
2.12 Computational Investigations on the Pathways Leading to Carbene	
Chapter 3. Summary and Outlook	36-38
3.1 Summary	
3.2 Outlook	
Chapter 4. Materials and Methods	39-48
4.1 General Methods	
4.1.1 Computational Details	
4.1.2 Experimental Details	
4.2 Theoretical Insights and Computational Methods	
4.2.1 History and Developments in Computational Chemistry	
4.2.2 Density Functional Theory (DFT)	
4.2.3 Basis Sets	
4.2.4 Bond Dissociation Energy (BDE)	
4.2.5 Natural Bond Orbital (NBO) Analysis	
4.3 Matrix Isolation Infrared Spectroscopy	
4.3.1 Technique and Experimental Setup	
4.3.2 Advantages of Matrix Isolation	
4.3.3 Limitations of Matrix Isolation	

4.3.4 Photochemical studies and bimolecular reactions under matrix conditions

4.3.5 Instrumental Setup

4.3.5.1 Cryostat

4.3.5.2 Helium Compressor

4.3.5.3 Temperature Controller

4.3.5.4 Vacuum System

4.3.5.5 FTIR Spectrometer

References 49-52

Appendix 53-65

LIST OF ABBREVIATIONS

TS:	Transition State
SB:	Singlet Biradical
TB:	Triplet Biradical
BDE:	Bond Dissociation Energy
ESP:	Electrostatic Potential
NBO:	Natural Bond Orbital
(U)B3LYP:	(Unrestricted) Becke, 3-parameter, Lee-Yang-Parr
(U)M06-2X:	(Unrestricted) Minnesota functional 06
cc-pVTZ:	Correlation Consistent Polarized Valence only basis set Triple-Zeta
PES:	Potential Energy Surface
(U)CCSD(T):	(Unrestricted) Coupled Cluster Single and Double Substitutions with triplets
SOMO:	Singly Occupied Molecular Orbital
DFT:	Density Functional Theory
(U)HF:	(Unrestricted) Hartree-Fock
CC:	Coupled Cluster
ESR:	Electron Spin Resonance
CIDNP:	Chemically Induced Dynamic Nuclear Polarization
CISD:	Configuration Interaction Single and Double Substitutions
PES:	Potential Energy Surface

LIST OF FIGURES

- Figure 1.1** Motivation and scope of current work
- Figure 1.2** System of Interest
- Figure 2.1** Geometrical optimization of **1**, **1O**, **1 α'** , **1 β** , **1 β'** and **1 γ**
- Figure 2.2** Geometrical optimization of **2**, **2O**, **2 α** , **2 α'** , **2 β'** and **2 γ**
- Figure 2.3** Geometrical optimization of **3**, **3O**, **3 α** and **3 β**
- Figure 2.4** Spin Density and SOMO of **1O**, **1 α'** , **1 β** , **1 β'** and **1 γ**
- Figure 2.5** Spin Density and SOMO of **2O**, **2 α** , **2 α'** , **2 β'** and **2 γ**
- Figure 2.6** Spin Density and SOMO of **3O**, **3 α** and **3 β**
- Figure 2.7** Electrostatic potential maps for parent and their respective isomeric radicals
- Figure 2.8** Nuclear independent chemical shift
- Figure 2.9** Isomerization channels through 1,2-H Shift
- Figure 2.10** Isomerization channels through 1,3-H Shift
- Figure 2.11** Deposition of 2-Iodo-hydroxy pyridine in argon matrix beyond 1800 cm⁻¹
- Figure 2.12** Photochemistry of 2-Iodo-hydroxy pyridine in argon matrix beyond 1800 cm⁻¹
- Figure 2.13** Photochemistry of 2-Iodo-hydroxy pyridine in argon matrix beyond 1800 cm⁻¹
- Figure 2.14** Photochemistry of 2-Iodo-hydroxy pyridine in argon matrix beyond 1800 cm⁻¹
- Figure 2.15** Photochemistry of 2-Iodo-hydroxy pyridine in argon matrix beyond 1800 cm⁻¹
- Figure 2.16** Ring opening pathway of **2 α**
- Figure 3.1** Summary and outlook
- Figure 4.1** Matrix Isolation FT-IR setup at POC lab
- Figure 4.2** Different parts of Matrix isolation setup

LIST OF TABLES

Table 2.1	Relative stability order of 1O , 1α' , 1β , 1β' and 1γ
Table 2.2	Relative stability order of 2O , 2α , 2α' , 2β' and 2γ
Table 2.3	Relative stability order of 3O , 3α and 3β
Table 2.4	Bond dissociation energy of 1O , 1α' , 1β , 1β' and 1γ
Table 2.5	Bond dissociation energy of 2O , 2α , 2α' , 2β' and 2γ
Table 2.6	Bond dissociation energy of 3O , 3α and 3β
Table 2.7	NBO analysis of 1β and 1γ
Table 2.8	NBO analysis of 1α' and 1β'
Table 2.9	NBO analysis of 2α and 2α'
Table 2.10	NBO analysis of 2β' and 2γ
Table 2.11	NBO analysis of 3α and 3β
Table 2.12	Isomerization channels through 1,2-H Shift
Table 2.13	Isomerization channels through 1,3-H Shift
Table 2.14	Singlet-triplet energy gap in di-dehydro-2-, 3-, 4-hydroxy pyridine biradical isomers
Table 2.15	Second BDE of di-dehydro-2-hydroxy pyridine biradical isomers
Table 2.16	Second BDE of di-dehydro-3-hydroxy pyridine biradical isomers
Table 2.17	Second BDE of di-dehydro-4-hydroxy pyridine biradical isomers
Table A1	Electronic and thermodynamic parameters of all the radical isomers
Table A2	Electronic and thermodynamic parameters of all the singlet and triplet biradical isomers
Table A3	Cartesian coordinates of the optimized structures

LIST OF SCHEMES

- Scheme 1.1** Phototchemistry of 2-Iodo-phenol
- Scheme 2.1** Possible dehydro-2-, 3-, 4-hydroxy pyridine radical isomers
- Scheme 2.2** Bond dissociation energies of radical isomers
- Scheme 2.3** Possible di- dehydro-2-, 3-, 4-hydroxy pyridine biradical isomers
- Scheme 2.4** Second bond dissociation energies of biradical isomers

Abstract

Phenoxy radical is one of the interesting transient and reactive species involved in various environmental and biological processes. It has also been reported as a key intermediate in the combustion processes of aromatic compounds. Moreover, simple and substituted phenoxy radical as metal-complexes play crucial roles in biocatalysis, redox reactions of proteins and electron-transfer reactions involving carotenoids. They also play a significant role in lignin biosynthesis, phenol-inhibited oxidation of hydrocarbons, and green plant photosynthesis. Despite the importance of phenoxy radical, direct observation and experimental studies on the heterocyclic analogues of them are scarce. In this regard, we adopted a strategy developed by Radziszewski and performed the photochemistry of 2-iodo-3-hydroxypyridine in argon matrices at 4 K in achieving the elusive 3-pyridyloxy radical. In line with the same literature report, instead of the expected target radical, we observed a ketene, arising due to the abstraction of the hydrogen by the iodine atom followed by Wolff rearrangement step. Now the situation is exciting because of the possibility of photogeneration of the prototypical *N*-heterocyclic carbene (NHC) with one heteroatom that has no substituent. So far, no reports are available with respect to the NHC without any substituent at the nitrogen centers. Considering the importance of NHC in variety of fields, such as catalysis, where the NHCs can either is used as an organocatalyst or as a ligand in making transition metal complexes. Through this work, matrix isolation infrared spectroscopic studies on 2-Iodo-3-hydroxy pyridine and relevant photochemistry and computational investigations on the isomeric pyridyloxy and hydroxypyridyl radicals are done.

Chapter 1: Introduction

1.1 Introduction to Free Radical Chemistry

Free radicals are one of the transient and important class of reactive intermediates^{1,2,3}. Free radical mechanism has a vital role to play in polymer^{4,5}, atmospheric^{6,7,8} and interstellar chemistry. With the growing advancement in chemistry, free radical pathways have attracted attention of many experimentalists and theoreticians. Equally, free radicals also have a huge role to play in understanding the ageing mechanism and diseases as from the biological point of view^{9,10}. Apart from this, several radical based reactions such as photoredox catalysis, radical addition and radical cyclization are of great importance in the field of organic synthesis^{11,12}.

From the basic science of stabilizing the radicals by electronic effects (i.e. inductive effect and resonance)^{13,14}, it was a challenge to stabilize this reactive intermediate for a large span of time. This challenge was soon overcome by the introduction of heteroatom in order to create stable radicals^{15,16,17}. In 1971, Hoffmann et al. came up with an explanation behind the driving force for the heteroatom based stable radicals¹⁸. The radical center is stabilized *via* (i) direct interaction between lone pair and radical (i.e. through space) and indirect interaction through intervening bonds (i.e. through bond)¹⁹. Equally, the creation of radical center at the heteroatom is an art to create stable radicals. The heteroatom centered radicals are stabilised by the flipping of the electron from σ -orbital of a radical center to π -orbital²⁰. Along with computational methods, many synthetic methods like radical traps²¹, radical clocks²² and experimental techniques such as electron spin resonance (ESR)²³, chemically induced dynamic nuclear polarization (CIDNP)²⁴, matrix isolation²⁵, mass spectrometry²⁶, photoelectron spectroscopy²⁷ and other spectroscopic techniques play a significant role in the better understanding of electronic structural and reactivity aspects.

1.2 Heterocyclic Radicals

Heterocyclic radicals are the radicals with a heteroatom in the ring. They have two main advantages in the electronic structure aspects. If the heterocyclic radical is a heteroatom centered, then it is more stable due to the delocalization of the radical in the π -cloud of the ring. Equally, if the radical is carbon centered then the radical is stabilized by the lone pair of

the heteroatom by through space (i.e. direct interaction) and through bond (interactions through intervening bonds) as discussed above. While looking into the reactivity aspects, the bond cleavage of heterocyclic radicals, but also their ring opening products and fragments play an important role in astrochemical point of view.

1.3 Phenoxy Radicals

Phenoxy radical is one of the interesting transient and reactive species involved in various environmental and biological processes. It has also been reported as a key intermediate in the combustion processes of aromatic compounds. Moreover, simple and substituted phenoxy radical as metal-complexes play crucial roles in biocatalysis²⁸, redox reactions of proteins²⁹. IR, UV-Vis, NMR and ESR studies of phenoxy radical has already been reported^{30,31}. Apart from this, kinetic behaviour and thermochemical properties of phenoxy radical have been explored. Literature reports on the oxidative coupling of phenolic compounds in the synthesis of natural products are of great importance³².

Various computational methods has helped in understanding the electronic structural parameter and the reactivity aspects of phenoxy radical³³. There are several reports of the synthesis of phenoxy radical, which are as follows (1)thermal decomposition pathway of anisole *via* cleavage of O-C bond led to the production of phenoxy radical³⁴. (2) Reaction of molecular oxygen with phenyl radical. In the combustion of aromatic hydrocarbons, phenoxy radical plays a valuable role as an intermediate. Despite the importance of phenoxy radical, direct observation and experimental studies on the heterocyclic analogues of them are scarce.

1.4 Motivation and Scope of the Current Work

Towards understanding the effect of heteroatom on reactivity and stability aspects, we have considered the isomeric analogues of hydroxyl pyridine, i.e., 2-hydroxy pyridine, 3-hydroxy pyridine and 4-hydroxy pyridine and their respective dehydro- radical isomers. All these groups, i.e., 2-hydroxy pyridine, 3-hydroxy pyridine and 4-hydroxy pyridine have five (**1O**, **1 α'** , **1 β** , **1 β'** , **1 γ**), five (**2O**, **2 α** , **2 α'** , **2 β'** , **2 γ**) and three (**3O**, **3 α** , **3 β**) possible radical isomers, respectively.

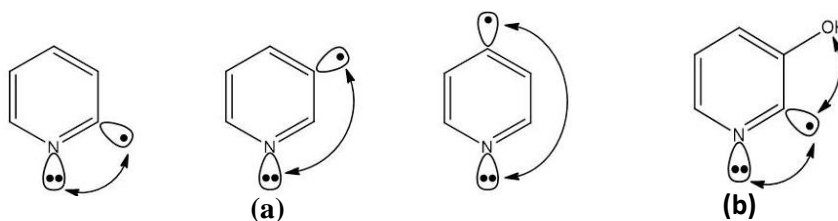


Figure 1.1: (a) Through Space (TS) and Through Bond (TB) interactions in pyridyl isomers. (b) Competitive lone pair radical interaction via oxygen and nitrogen lone pairs.

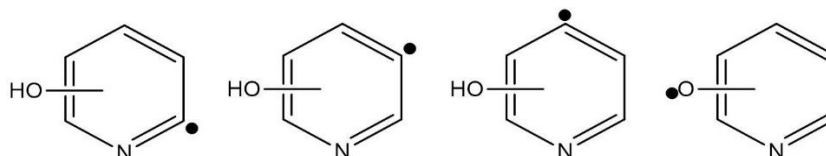
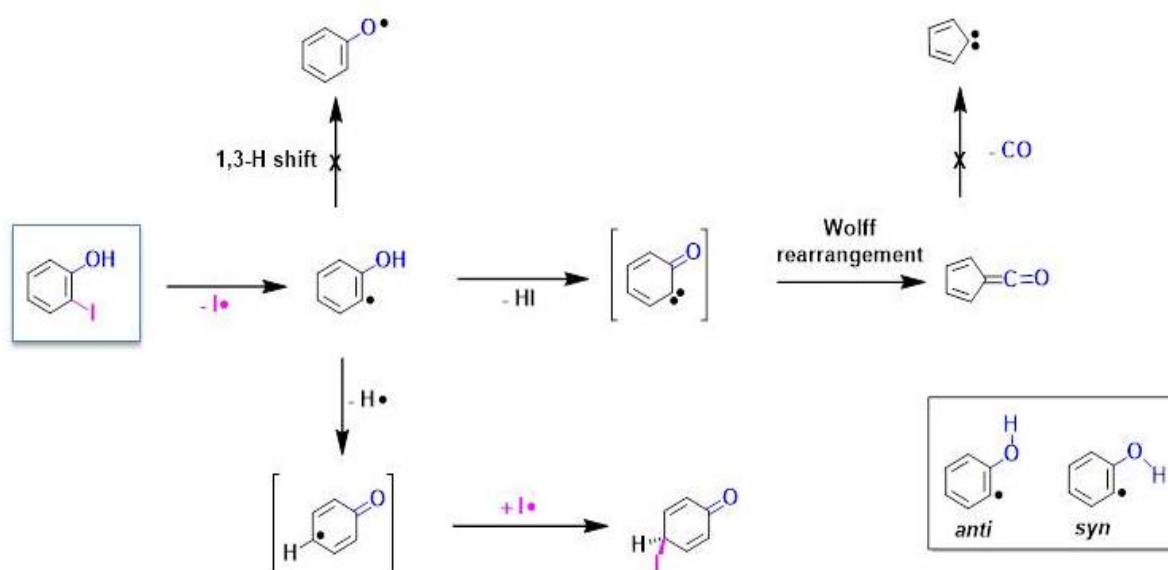


Figure 1.2: System of interest, i.e., 2-hydroxy pyridine, 3-hydroxy pyridine and 4-hydroxy pyridine and their respective dehydro- radical isomers.

Along with the computational part of the investigations on all the possible hydroxypyridine derived radicals, we have considered the 2-dehydro-3-hydroxypyridine radical as an experimental target. The reason is the potential formation of 3-pyridyloxy radical through 1,3-H shift. In this regard, we adopted a strategy developed by Radziszewski's group (Figure 1.3) and performed the photochemistry of 2-iodo-3-hydroxypyridine in argon matrices at 4 K in achieving the elusive 3-pyridyloxy radical³⁵. In line with the same literature report, instead of the expected target radical, we observed a ketene, arising due to the abstraction of the hydrogen by the iodine atom followed by Wolff rearrangement step. Now the situation is exciting because of the possibility of photogeneration of the prototypical N-heterocyclic carbene (NHC) with one heteroatom that has no substituent. So far, no reports are available with respect to the NHC without any substituent at the nitrogen centers. Considering the importance of NHC in variety of fields, such as catalysis, where the NHCs can either be used as an organocatalyst or as a ligand in making transition metal complexes^{36,37,38,39}.



Scheme 1.1: Photochemistry of 2-Iodo-phenol by Radziszewski and group.

1.5 Approaches

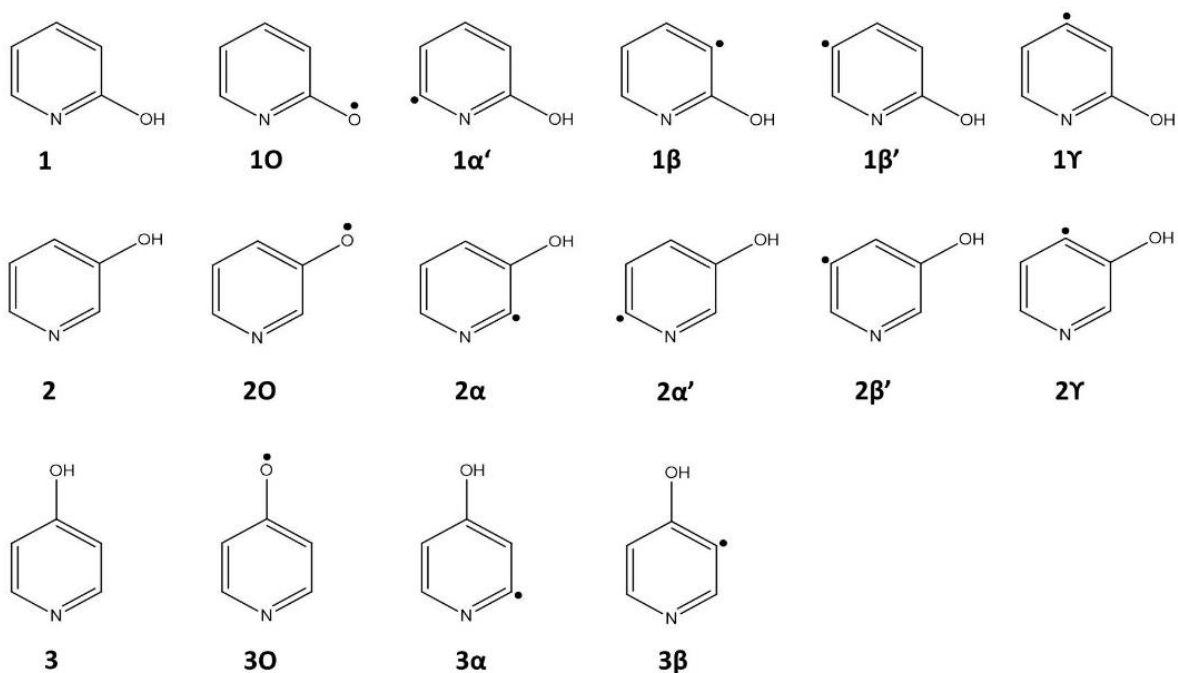
To understand the electronic structural aspects of dehydro- 2-, 3- and 4-hydroxy pyridine radical isomers, DFT computations have been used. In this regard, we explored the ground state electronic structures and their geometrical parameters to get insights in to the structural aspects. Spin density and electrostatic potentials (ESP) have been computed in order to understand the localization of spin at the radical center, and to get an overview of the electrostatic charges, respectively. Natural bond orbital (NBO) analysis has been performed for obtaining semi-quantitative information on the interaction between lone pair(s) of the heteroatom and radical electron. Similarly to understand biradicals, singlet-triplet energy gap and bond dissociation energy calculations were performed. The matrix isolation infrared spectroscopy technique has been used for the confirmation of our radical of interest (i.e. 2-dehydro-3-hydroxy pyridyl radical) and its photoproducts.

Chapter 2: Results and Discussion

Computational studies of isomeric pyridyloxy and hydroxyl pyridyl radicals have been carried out in order to observe the effect of heteroatoms (N and O) in stabilizing the radicals through lone pair-radical interactions. In this regard, we explored the electronic structural and stability aspects. Apart from this, reactivity aspects of these radicals were explored by studying several mechanistic pathways such as, (i) 1,2 and 1,3 H-shift (isomerization). (ii) Biradical formation by calculating second bond dissociation energies. (iii) Unimolecular decomposition channels of the radicals resulting in ring opening products. Photochemistry of 2-IHP radical has also been performed under 4 K using matrix isolation infrared spectroscopy technique. The outcomes of these studies are discussed in detail.

2.1 System of Interest

The isomeric hydroxy pyridine and their respective radical analogues (i.e. target radicals) have been computed at different levels of theory (Scheme 2.1). The objective behind this was to generalize the effect of heteroatom in stabilizing the radicals. Interestingly, there can be a potential competition between the nitrogen as well as oxygen lone pair of hydroxy group in imparting stability. For the better understanding of the interactive forces between the lone pair and the radical center, NBO analysis have also been performed at (U)B3LYP/cc-pVTZ level of theory. The nomenclature is done in 3 groups such as 1, 2, 3 corresponding to the 2-, 3-, 4-hydroxy pyridine. The oxygen centered radicals are named as **1O**, **2O**, **3O** which corresponds to 2-, 3-, 4-hydroxy pyridyloxy radicals. For the carbon centered radicals, the nomenclature is done with respect to the nitrogen center, radical center positioned at *ortho* is α and α' whereas, *meta* is β and β' and *para* is γ . The prime here implies to the radical center opposite to the hydroxyl group.



Scheme 2.1: Parent hydroxy pyridines and their isomeric radicals

2.2 Geometrical Parameters

The structures were optimised along with their geometrical parameters for the parent molecule, and their isomeric radical analogues as shown in figure 2.2, 2.3, 2.4. All the optimized geometries have been confirmed by frequency calculations for ensuring the minimum energy structures on the potential energy surface. All the molecules were optimized in either C_{2v} or C_s point group symmetries and possess a spin doublet. We compared features like the bond length, bond angle and the planarity of the various radicals with their parent molecule. On analysis, we observed that all these radicals follow some general trends. (i) The bonds lengths just adjacent to the radical centre got shortened, whereas alternate bond lengths relative to radical centre got increased as compared to the parent. (ii) We also observed that the bond angle at the carbon centre increases, whereas it decreases in the case of nitrogen centered radicals as compared to their respective parent. The geometrical parameters for both parent as well as their respective radicals have been estimated at both (U)B3LYP/cc-pVTZ and (U)M06-2X/cc-pVTZ levels of theory and the results were consistent with both the levels.

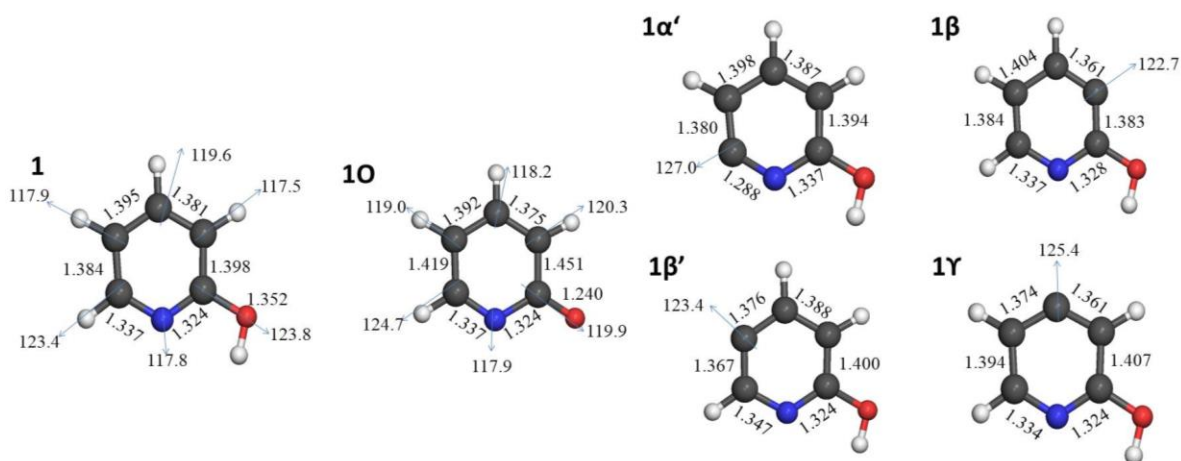


Figure 2.1: Geometrical optimization of parent **1** (C_s symmetry), **1O** (C_s symmetry), **1 α'** (C_s symmetry), **1 β** (C_s symmetry), **1 β'** (C_s symmetry) and **1 γ** (C_s symmetry) at (U)B3LYP/cc-pVTZ level of theory. At the radical centers, the bond distances and the bond angles are mentioned in Å units and in degrees respectively.

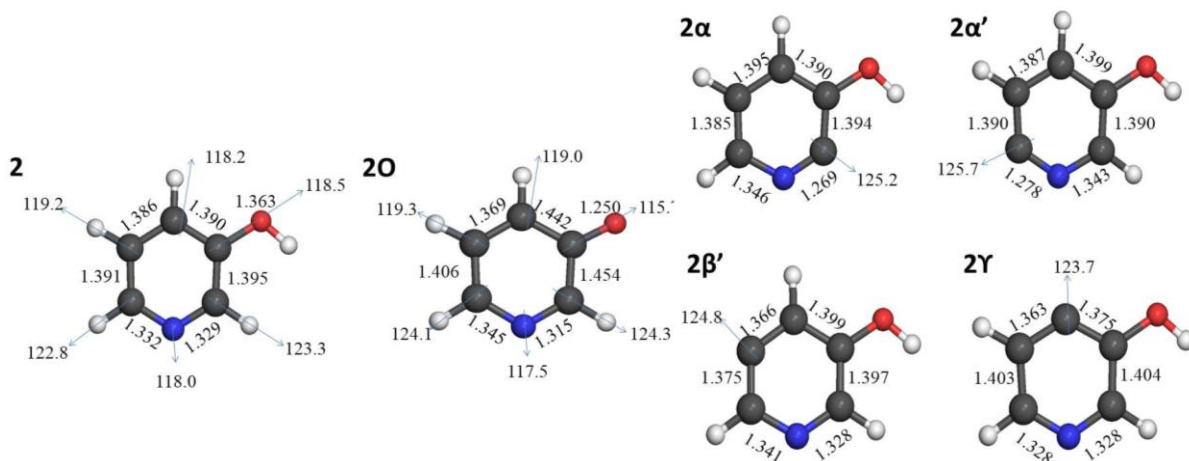


Figure 2.2: Geometrical optimization of parent **2** (C_s symmetry), **2O** (C_s symmetry), **2 α** (C_s symmetry), **2 α'** (C_s symmetry), **2 β'** (C_s symmetry) and **2 γ** (C_s symmetry) at (U)B3LYP/cc-pVTZ level of theory. At the radical centers, the bond distances and the bond angles are mentioned in Å units and in degrees respectively.

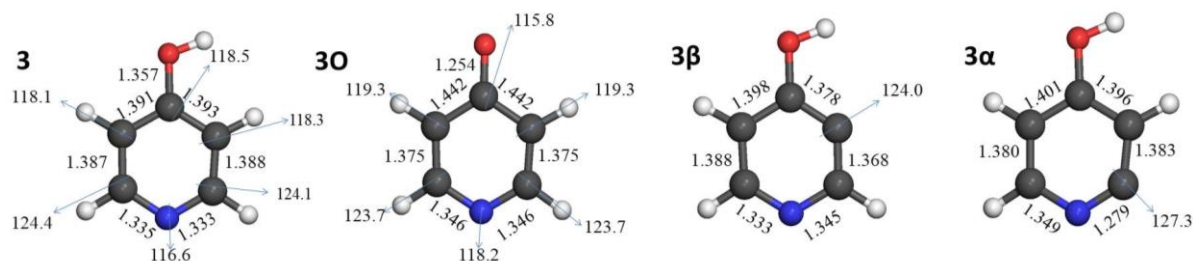


Figure 2.3: Geometrical optimization of parent **3** (C_s symmetry), **3O** (C_{2v} symmetry), **3 α** (C_s symmetry) and **3 β** (C_s symmetry) at (U)B3LYP/cc-pVTZ level of theory. At the radical centers, the bond distances and the bond angles are mentioned in Å units and in degrees respectively.

2.3 Stability Order of Monoradicals

During our study, we explored 13 radicals, out of which 3 were oxygen centered and 10 being carbon centered. For a better understanding, we compared the oxygen centered as well as carbon centered radicals separately within three groups. The early studies of pyridyl radicals from our group had the stability order: *ortho*>*para*>*meta*. We were keenly interested to figure out the stability order as there is a potential competition between the lone pair of oxygen and nitrogen for imparting the stability to the radical centre. Optimization and frequency calculations for all the radicals with their conformers (i.e. *syn* and *anti*) have been performed at different levels of theory. The *syn* conformer was found to be more stable than its *anti* form, which clearly indicates that oxygen lone pair may have a repulsive interaction with the radical center. The oxygen centered radicals were more stable than their carbon centered counterparts. The higher stability of oxygen centered radicals can be attributed to the delocalisation of radical electron over the ring. The relative stability of C-centered radicals were explained on the basis of NBO interactions. NBO analysis also showed the dominating stabilisation of radical center through nitrogen lone pair rather than the oxygen lone pair.

In order to understand the relative stability pattern based on absolute energy, the isomeric radical species for 2-, 3-, 4- hydroxy pyridine groups have been estimated at different levels of theory and their relative energies are listed in the **table 2.1**. Out of all the above-mentioned radicals, **1 α '**, **1 β** , **1 β '**, **1 γ** , **2 α** , **2 α '**, **2 β '**, **2 γ** , **3 α** , **3 β** are carbon centered, which differs with respect to their relative positioning from the heteroatom (**1O**, **2O**, **3O**). In case of 2-hydroxy pyridine group radicals **1O** has minimum energy and was found to be the most stable isomer followed by **1 α '**, **1 γ** , **1 β** , **1 β '**, where **1 β** , **1 β '** are very close in energy with an energy difference ranging between 0.0 to 0.3 kcal/mol depending on the levels of theory. Different levels of theory predicted different relative energies trend for **1 β** and **1 β '**. In case of 3-hydroxy pyridine group radicals, **2O** has minimum energy and was found to be the most stable isomer followed by **2 α** , **2 α '**, **2 β '**, **2 γ** . Different levels of theory predicted different relative energies trend for **2 β '** and **2 γ** . In case of 4-hydroxy pyridine group radicals, **3O** was found to be the most stable followed by **3 α** , which is more stable as compared to **3 β** with an energy difference ranging between 6.7 to 7.0 kcal/mol at (U)B3LYP/cc-pVTZ and (U)MO6-2X/cc-pVTZ levels of theory. Within the groups, the higher stability of oxygen centered radicals can be attributed to the delocalisation of radical center over the ring. All the levels of theory follow the same trend in case of 2-, 3-, 4- hydroxy pyridyl radicals. Slight variations

were observed in case of isomers **1 β** and **1 β'** , **2 β'** and **2 γ** isomers at (U)M06-2X/cc-pVTZ and single point energy calculation performed at CCSD(T)/cc-pVTZ//(U)B3LYP/cc-pVTZ levels as shown in the Table 2.1.

Table 2.1: Relative stability order of **1O**, **1 α'** , **1 β** , **1 β'** , and **1 γ** in kcal/mol at different level of theory and at basis set cc-pVTZ (Bold font: *syn* isomer; Italics: *anti* form)

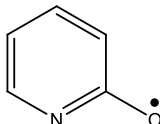
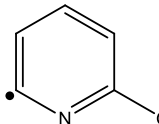
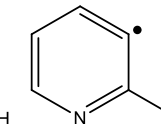
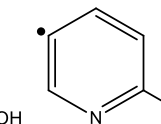
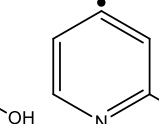
Levels of Theory					
	1O	1α'	1β	1β'	1γ
(U)B3LYP	0.0	12.4	21.4	24.0	21.5
		<i>16.4</i>	<i>19.0</i>	<i>19.3</i>	<i>16.8</i>
(U)M06-2X	0.0	7.7	17.7	19.3	16.4
		<i>12.0</i>	<i>14.7</i>	<i>14.4</i>	<i>11.5</i>
(U)CCSD(T)	0.0	7.1	13.1	14.5	14.4
		<i>12.5</i>	<i>9.0</i>	<i>9.0</i>	<i>9.0</i>

Table 2.2: Relative stability order of **2O**, **2 α** , **2 α'** , **2 β'** and **2 γ** in kcal/mol at different level of theory and at basis set cc-pVTZ (Bold font: *syn* isomer; Italics: *anti* form)

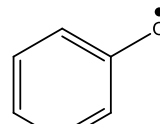
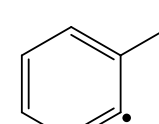
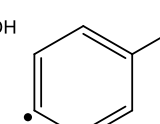
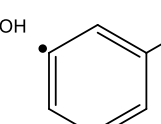
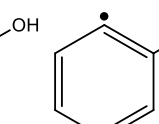
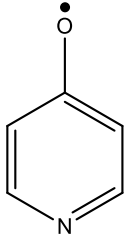
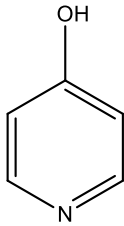
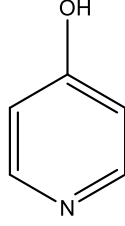
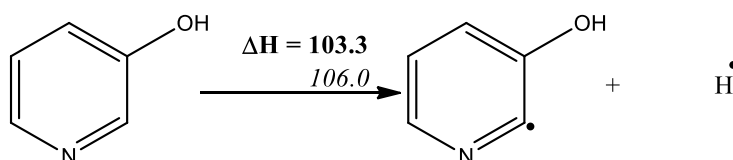
Levels of Theory					
	2O	2α	2α'	2β'	2γ
(U)B3LYP	0.0	18.6	21.9	26.4	26.0
		<i>21.2</i>	<i>21.5</i>	<i>26.0</i>	<i>27.3</i>
(U)M06-2X	0.0	15.4	18.1	22.6	22.0
		<i>17.8</i>	<i>17.6</i>	<i>22.2</i>	<i>23.1</i>
(U)CCSD(T)	0.0	13.6	3.1	7.4	6.4
		<i>2.2</i>	<i>14.9</i>	<i>15.9</i>	<i>17.4</i>

Table 2.3: Relative stability order of **3O**, **3 α** and **3 β** in kcal/mol at different level of theory and at basis set cc-pVTZ (Bold font: *syn* isomer; Italics: *anti* form)

Levels of Theory			
	3O	3α	3β
(U)B3LYP	0.0	14.5	21.2
		<i>14.9</i>	<i>22.9</i>
(U)M06-2X	0.0	9.6	16.7
		<i>9.9</i>	<i>18.1</i>
(U)CCSD(T)	0.0	11.6	13.1
		<i>2.6</i>	<i>4.8</i>

2.4 Bond Dissociation Energy (BDE)

Bond dissociation energies is defined as the change in the enthalpy accompanied in a reaction during homolytic cleavage of C-H or O-H bond leading to the formation of radical and hydrogen atom. In order to confirm the relative stability order, BDE calculation have been performed at (U)B3LYP/cc-pVTZ level of theory. BDE value plays a significant role in explaining the thermodynamic stability of the radical. The higher stability of oxygen centered radicals than their carbon centered counterparts are also reflected in their lower BDE values. The schematic picture of the first bond dissociation of the parent molecule is shown in Scheme 2.2 and the values for first BDE's are tabulated in table 2.4 at different levels of theory. The BDE order was found to be consistent with the relative stability order.



Scheme 2.2: First bond dissociation energy of the molecule

Table 2.4: The first C–H BDEs in kcal/mol of the 2-hydroxy pyridine molecules leading to the dehydro-2-hydroxy pyridyl radicals (**bold**: *syn* isomer; *italics*: *anti* form).

Reactant	Product	First BDE (kcal/mol)
Parent 1	1O + H [•]	93.6
Parent 1	1α' + H [•]	106.0
		<i>110.0</i>
Parent 1	1β + H [•]	115.0
		<i>112.6</i>
Parent 1	1β' + H [•]	117.6
		<i>112.9</i>
Parent 1	1γ + H [•]	115.1
		<i>112.6</i>

Table 2.5: The first C–H BDEs in kcal/mol of the 3-hydroxy pyridine molecules leading to the dehydro-3-hydroxy pyridyl radicals (**bold**: *syn* isomer; *italics*: *anti* form).

Reactant	Product	First BDE (kcal/mol)
Parent 2	2O + H [•]	84.8
Parent 2	2α' + H [•]	106.7
		<i>106.3</i>
Parent 2	2α + H [•]	103.3
		<i>106.0</i>
Parent 2	2β' + H [•]	111.1
		<i>110.7</i>
Parent 2	2γ + H [•]	110.8
		<i>112.1</i>

Table 2.6: The first C–H BDEs in kcal/mol of the 4-hydroxy pyridine molecules leading to the dehydro-4-hydroxy pyridyl radicals (**bold**: *syn* isomer; *italics*: *anti* form).

Reactant	Product	First BDE (kcal/mol)
Parent 3	2O + H [•]	90.3
Parent 3	2α + H [•]	104.8 <i>105.2</i>
Parent 3	2β + H [•]	111.5 <i>113.3</i>

2.5 Spin Density

Spin density is defined as the electron density of one spin (beta spin) subtracted from the electron density of the opposite spin (alpha spin). Analysis of spin density illustrates how the electron spin at the radical centre is distributed whether it is localized or delocalized and also provides qualitative information about the interaction of radical electron with other atoms. The spin density of all the radical isomers have been estimated at (U)B3LYP/cc-pVTZ and (U)M06-2X/cc-pVTZ levels of theory and the results are shown in figure 3.2. The observations depict that all the carbon centered radicals (**1 α'** , **1 β** , **1 β'** , **1 γ** , **2 α** , **2 α'** , **2 β'** , **2 γ** , **3 α** , **3 β**) carries a large positive spin density value at the formal radical centers, which suggests that these radical spins are localized. On the other hand, the *O*-centered radical (**1O**, **2O**, **3O**) showed a different trend. These spin density values for *O*-centered radicals implies that the spin density and the resulting radical character is delocalized over the ring. The higher spin density at formal radical centers can be expected to have higher reactivity. The relative stability order was found to be consistent with spin density trend for all the radical isomers. However, these radicals comprise spin densities with negligible difference, which is acceptable as the relative energy differences among these radicals are trivial. The greater degree of stabilization in **1O**, **2O**, **3O** can also be explained using the distribution of spin and radical character throughout the molecule.

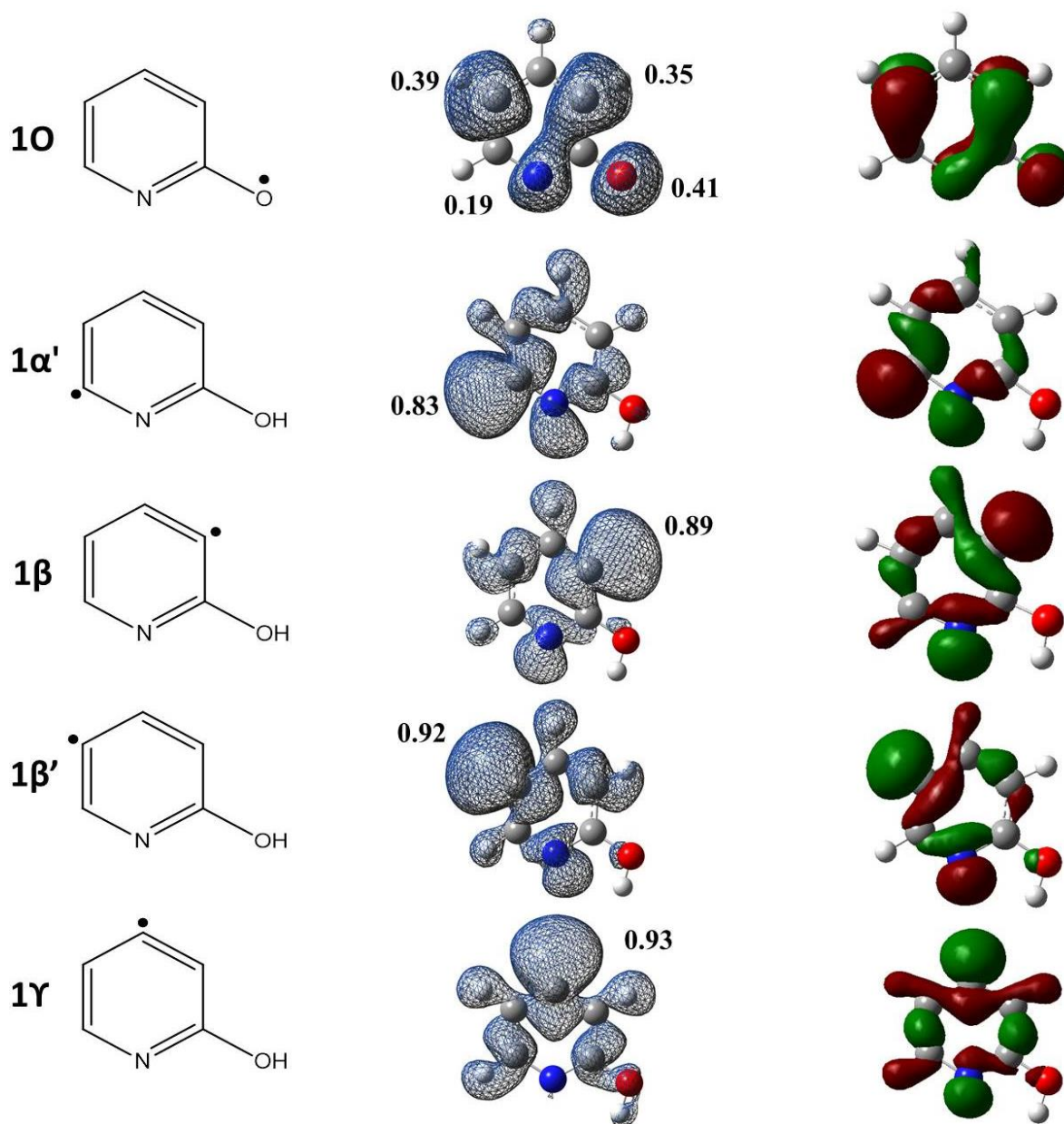


Figure 2.4: Spin density values and SOMO (singly occupied molecular orbital, rendered at an isovalue 0.05) of $1O$, $1\alpha'$, 1β , $1\beta'$ and 1γ at (U)B3LYP/cc-pVTZ level of theory.

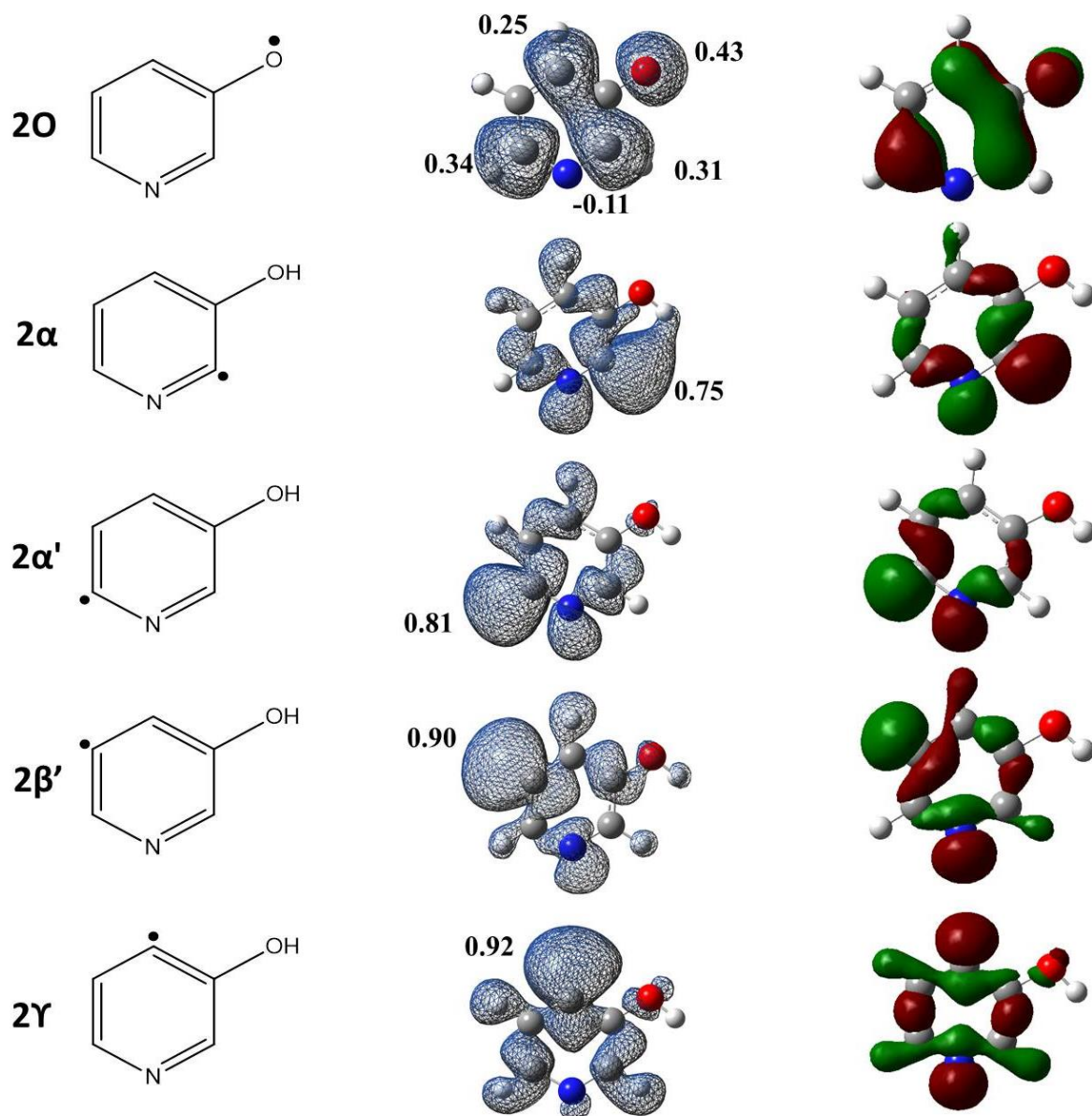


Figure 2.5: Spin density values and SOMO (singly occupied molecular orbital, rendered at an isovalue 0.05) of **2O**, **2 α** , **2 α'** , **2 β'** and **2 γ** radical center at (U)B3LYP/cc-pVTZ level of theory.

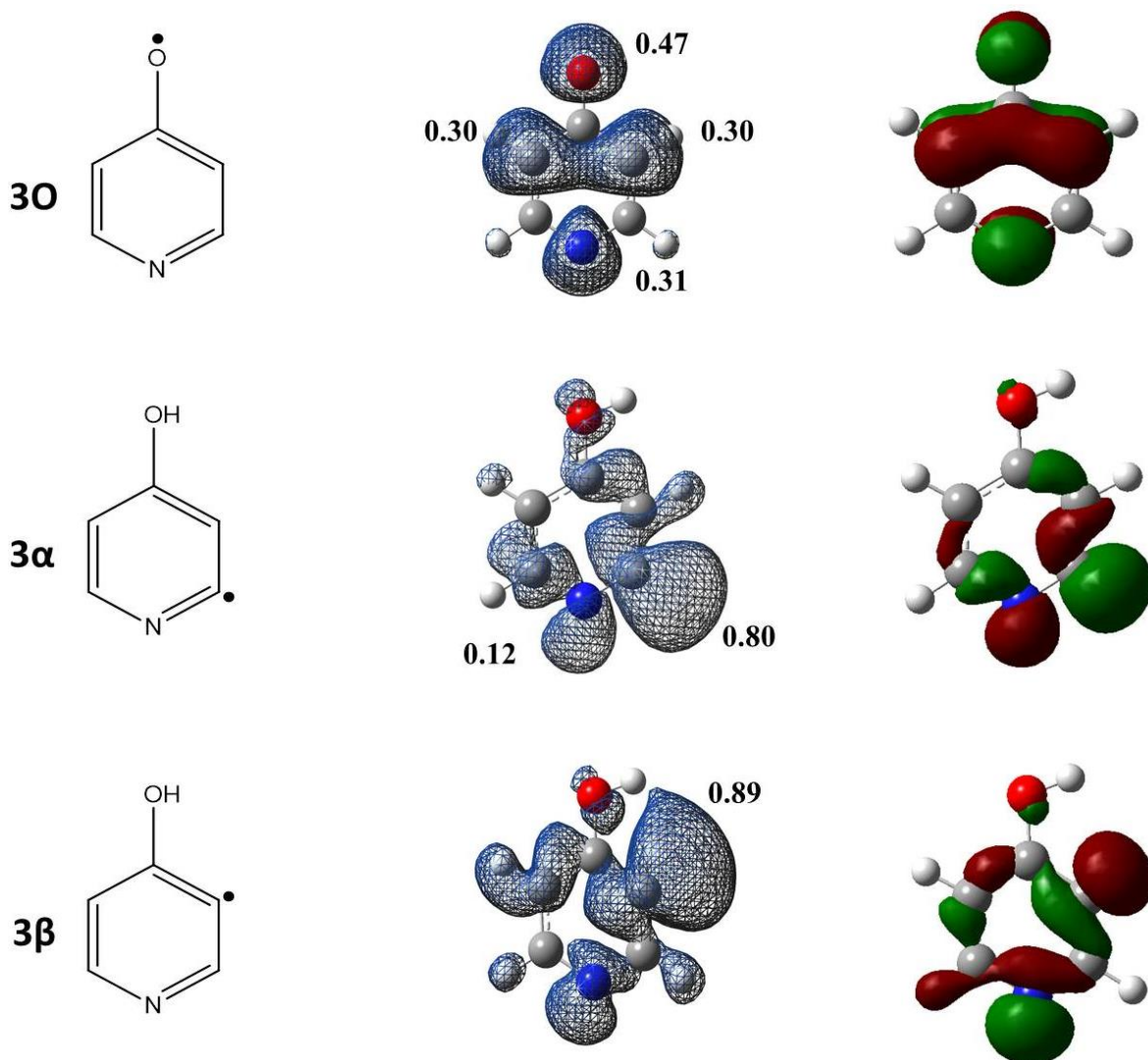


Figure 2.6: Spin density values and SOMO (singly occupied molecular orbital, rendered at an isovalue 0.05) of **3O**, **3 α** and **3 β** radical center at (U)B3LYP/cc-pVTZ level of theory.

2.6 Electrostatic Potential (ESP)

Electrostatic potential (ESP) is a mapping, which helps in understanding the charge distribution and other charge related properties of the molecule. ESP surface plays an important role in identification of electron rich and deficient regions according to the colour variation. ESP mapping is also useful to understand the nature of chemical bond. Qualitative estimation of bond polarization can be very well interpreted by the extent of positive and negative potentials between the atoms. In this regard, the three dimensional potential mapping of all the radical isomers and their respective parent molecules are generated and plotted in figure 2.8. The mapping clearly indicates a negative potential over nitrogen and oxygen atom due to the presence of lone pair of electrons. Creation of radical center at

oxygen enhances the negative potential to greater extent. Similarly radical center also depicts a negative potential for all the carbon centered radical as expected, which also confirms the results from spin density calculations.

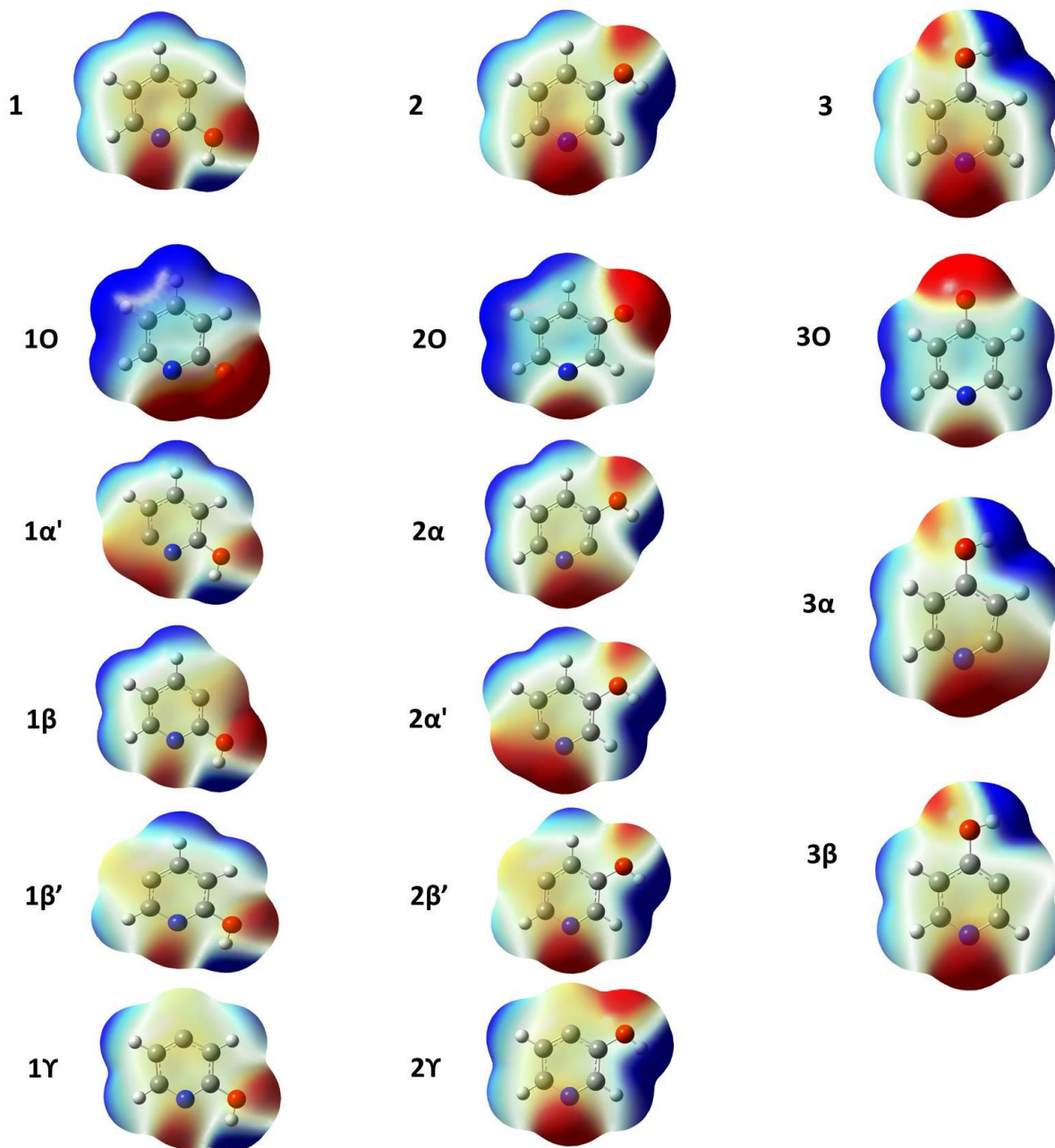


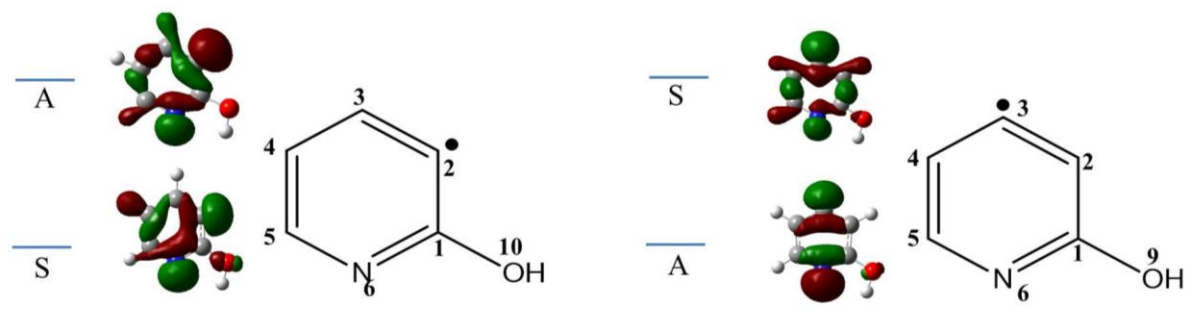
Figure 2.7: Electrostatic potential map for 2-, 3-, 4- hydroxyl pyridine and their respective isomeric radicals at (U)B3LYP/cc-pVTZ level of theory.

2.7 Natural Bond Orbital (NBO) Analysis

NBO Analysis was mainly used in quantification of lone pair (if available) – radical interactions. The energies corresponding to the interacting orbitals depend upon the energy difference between the donor and acceptor orbitals. The interaction energies of the various donor–acceptor orbital interactions for the various carbon-centered radicals at (U)B3LYP/cc-pVTZ level of theory has been tabulated in tables below. NBO calculation was restricted to only carbon centered radicals, because the energy estimation is only possible for the localised radical at their respective centers. Contrary to this, oxygen centered radicals stabilisation could not be figured due to the delocalisation of the radical centre.

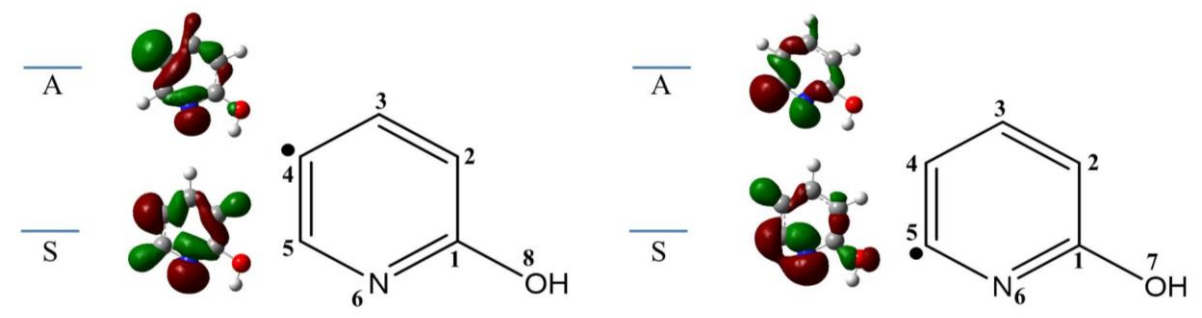
Through these studies, we mainly focused on the interactions between the lone pair and the radical electron and their mode of interaction, i.e. through space (direct interaction) or through bond (indirect interactions through intervening bonds). In order to figure out the results obtained from NBO analysis, we also looked into the molecular orbitals (i.e. low lying lone pair and SOMO) for all the possible carbon-centered radicals. In general, when the interacting orbitals are *ortho* to each other, TS (through space) interaction will be more dominant; while for the *para* position TB (through bond) interactions governs the stability. For the *meta* position, the interacting orbitals have minimal amount of both TS and TB interactions. Hoffmann provided a qualitative description of TS and TB interactions by symmetric and antisymmetric combinations of the two interacting orbitals.⁽¹⁹⁾ For the TS interactions, the low lying lone pair orbital is symmetric and the singly occupied molecular orbital (SOMO) is antisymmetric. On the other hand, the low lying lone pair orbital is antisymmetric and the radical orbital (SOMO) is symmetric for TB interactions.

Table 2.7: NBO interaction energy for **1 β** and **1 γ** at (U)B3LYP/cc-pVTZ level of theory along with their MOs (molecular orbitals) rendered at an isovalue of 0.05.



1β			1γ		
Interactions			Interactions		
Donor NBO	Acceptor NBO	E	Donor NBO	Acceptor NBO	E
$\pi_{1(C3-C4)}$	$n_{1(C2)}^*$	6.10	$\pi_{1(C1-C2)}$	$n_{1(C3)}^*$	7.44
$\pi_{1(C3-H7)}$	$n_{1(C2)}^*$	1.26	$\pi_{1(C4-C5)}$	$n_{1(C3)}^*$	7.72
$n_{1(N6)}$	$n_{1(C2)}^*$	0.79	$\pi_{1(C4-H7)}$	$n_{1(C3)}^*$	0.62
$n_{1(N6)}$	$\pi_{1(C1-C2)}^*$	6.50	$\pi_{2(C1-N6)}$	$\pi_{2(C4-C5)}^*$	15.21
$n_{2(O10)}$	$\pi_{2(C1-N6)}^*$	18.12	$\pi_{2(C4-C5)}^*$	$\pi_{2(C2-C3)}^*$	37.51
$\pi_{2(C1-N6)}^*$	$\pi_{2(C2-C3)}^*$	33.29	$n_{2(O9)}$	$\pi_{2(C1-N6)}^*$	18.85
			$\pi_{2(C1-N6)}^*$	$\pi_{2(C2-C3)}^*$	25.64

Table 2.8: NBO interaction energy for **1 α'** and **1 β'** at (U)B3LYP/cc-pVTZ level of theory along with their MOs (molecular orbitals) rendered at an isovalue of 0.05.



1β'			1α'		
Interactions			Interactions		
Donor NBO	Acceptor NBO	E	Donor NBO	Acceptor NBO	E
$\pi_{1(C2-C3)}$	$n_{1(C4)}^*$	6.20	$\pi_{1(C3-C4)}$	$n_{1(C5)}^*$	7.40
$\pi_{1(C5-N6)}$	$n_{1(C4)}^*$	4.52	$\pi_{1(C1-N6)}$	$n_{1(C5)}^*$	4.96
$\pi_{1(C5-H7)}$	$n_{1(C4)}^*$	0.64	$\pi_{1(C4-C5)}$	$n_{1(C5)}^*$	0.53
$n_{1(N6)}$	$n_{1(C4)}^*$	0.69	$n_{1(N6)}$	$n_{1(C5)}^*$	16.65
$n_{1(N6)}$	$\pi_{1(C4-C5)}^*$	5.22	$n_{1(N6)}$	$\pi_{1(C4-C5)}^*$	3.25
$n_{2(O8)}$	$\pi_{2(C1-N6)}^*$	17.52	$n_{2(O7)}$	$\pi_{2(C1-C2)}^*$	17.20
$\pi_{2(C1-N6)}^*$	$\pi_{2(C4-C5)}^*$	24.27	$\pi_{2(C1-C2)}^*$	$\pi_{2(C5-N6)}^*$	36.19

Table 2.9: NBO interaction energy for 2α and $2\alpha'$ at (U)B3LYP/cc-pVTZ level of theory along with their MOs (molecular orbitals) rendered at an isovalue of 0.05.

$2\alpha'$			2α		
Interactions			Interactions		
Donor NBO	Acceptor NBO	E	Donor NBO	Acceptor NBO	E
$\pi_{1(C3-C4)}$	$n_{1(C5)}^*$	6.52	$\pi_{1(C2-C3)}$	$\pi_{2(C1-N6)}^*$	4.49
$\pi_{1(C1-N7)}$	$n_{1(C5)}^*$	4.63	$\pi_{1(C1-N6)}$	$\pi_{1(C1-C2)}^*$	0.78
$\pi_{1(C1-N7)}$	$\pi_{1(C4-C5)}^*$	0.31	$\pi_{1(C4-C5)}$	$\pi_{2(C1-N6)}^*$	0.62
$n_{1(N7)}$	$n_{1(C5)}^*$	21.16	$n_{2(O7)}$	$\pi_{1(C1-C2)}^*$	3.44
			$n_{2(O7)}$	$\pi_{2(C2-C3)}^*$	14.53
			$\pi_{2(C2-C3)}^*$	$\pi_{3(C1-N6)}^*$	51.33

Table 2.10: NBO interaction energy for $2\beta'$ and 2γ at (U)B3LYP/cc-pVTZ level of theory along with their MOs (molecular orbitals) rendered at an isovalue of 0.05.

2γ			$2\beta'$		
Interactions			Interactions		
Donor NBO	Acceptor NBO	E	Donor NBO	Acceptor NBO	E
$\pi_{1(C1-C2)}$	$n_{1(C3)}^*$	7.28	$\pi_{1(C2-C3)}$	$n_{1(C4)}^*$	6.10
$\pi_{1(C4-C5)}$	$n_{1(C3)}^*$	6.88	$\pi_{1(C5-N8)}$	$n_{1(C4)}^*$	5.14
$\pi_{1(C4-H7)}$	$n_{1(C3)}^*$	1.19	$\pi_{1(C4-C5)}$	$n_{1(C5)}^*$	0.53
			$n_{1(N8)}$	$n_{1(C4)}^*$	0.81
			$\pi_{1(C5-H7)}$	$n_{1(C4)}^*$	0.35
			$\pi_{1(C3-H11)}$	$n_{1(C4)}^*$	1.08

Table 2.11: NBO interaction energy for **3 α** and **3 β** at (U)B3LYP/cc-pVTZ level of theory along with their MOs (molecular orbitals) rendered at an isovalue of 0.05.

3β			3α		
Interactions			Interactions		
Donor NBO	Acceptor NBO	E	Donor NBO	Acceptor NBO	E
$\pi_{1(C2-C3)}$	$n_{1(C4)}^*$	6.23	$\pi_{2(C1-C2)}$	$\pi_{2(C5-N8)}^*$	4.83
$\pi_{2(C2-C3)}$	$\pi_{2(C4-C5)}^*$	9.32	$\pi_{2(C3-C4)}$	$\pi_{2(C5-N8)}^*$	15.77
$\pi_{2(C1-N9)}$	$\pi_{2(C4-C5)}^*$	10.72	$\pi_{1(C3-C4)}$	$n_{1(C5)}^*$	6.44
$\pi_{1(C5-H8)}$	$n_{1(C4)}^*$	0.69	$n_{1(N8)}$	$n_{1(C5)}^*$	20.17
$n_{1(N9)}$	$n_{1(C4)}^*$	0.98	$n_{1(N9)}$	$\pi_{1(C4-C5)}^*$	3.39
$n_{1(N9)}$	$\pi_{1(C4-C5)}^*$	5.77	$n_{2(O9)}$	$\pi_{2(C3-C4)}^*$	16.49
$n_{1(O10)}$	$n_{1(C4)}^*$	0.42	$\pi_{2(C3-C4)}^*$	$\pi_{2(C5-N8)}^*$	33.68
$n_{2(O10)}$	$\pi_{2(C2-C3)}^*$	14.65			
$\pi_{2(C2-C3)}^*$	$\pi_{2(C4-C5)}^*$	45.52			

2.8 Nuclear Independent Chemical Shift (NICS)

Nuclear Independent Chemical Shift (NICS) is a useful method for the understanding the aromatic, antiaromatic and non-aromatic character of a molecule. In general, probe atom is placed at the centre of the heterocyclic ring and its position is varied perpendicular to the molecular plane (i.e. from 0.0 Å to 2.0 Å). The ring current around the probe atoms gives the magnetic shielding values, negative of this magnetic shielding gives the NICS value. The highly negative NICS value indicates that the molecule is aromatic (i.e. diatropic ring current) in nature, whereas a positive value shows antiaromaticity (i.e. paratropic ring current). NICS ranging between highly negative and positive value is an indication of nonaromatic molecule. NICS for all the heterocyclic parent and their isomeric radicals have been estimated at (U)B3LYP/cc-pVTZ level of theory and their NICS(1.0) values are given in figure 2.9. On comparing the NICS values, parent molecule had more aromatic character than their respective radicals. All the π -delocalised oxygen centered radical has lower NICS value, which can be attributed to the loss of aromaticity (i.e. Huckel's rule). Interestingly, few hydroxypyridyl radicals (**1 γ** , **1 α'** , **2 γ** , **2 β'** , **2 α** , **2 α'** , **3 α**) showed more negative NICS value as compared to their respective parent molecules.

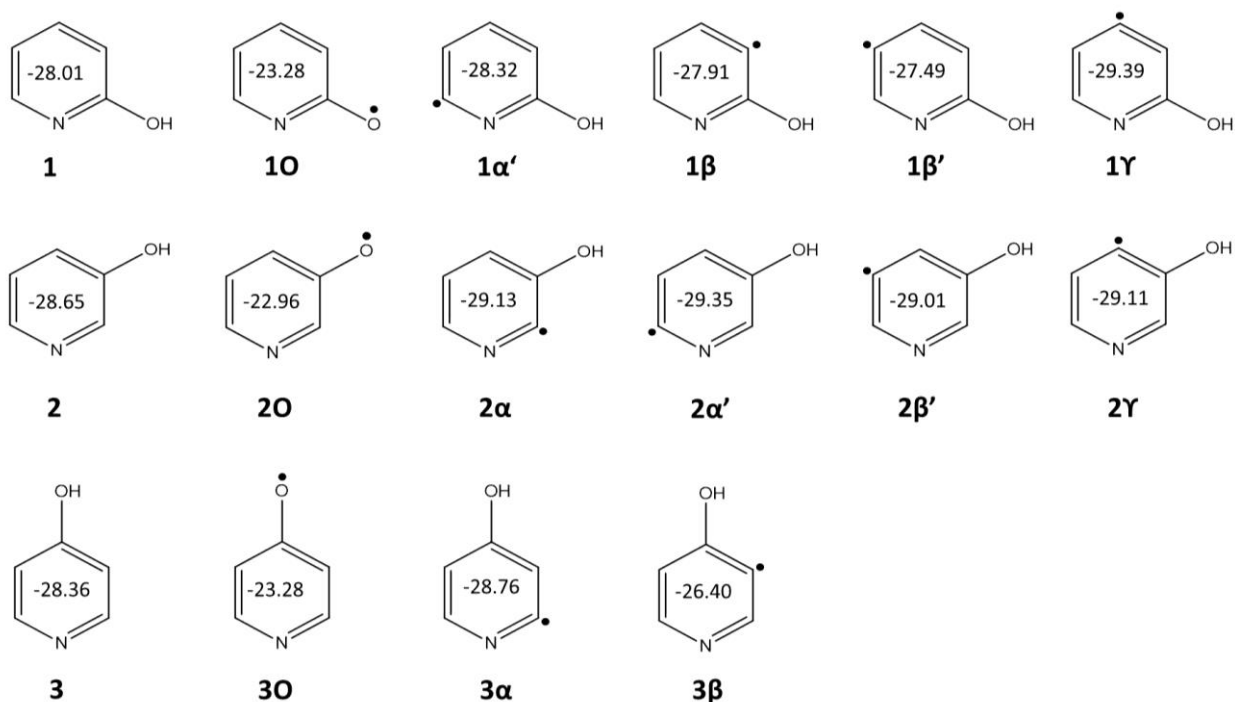


Figure 2.8: NICS (1.0) indices for 2-, 3-, and 4-hydroxy pyridine and their corresponding radical isomers performed at the (U)B3LYP/cc-pVTZ level of theory

2.9 Reactivity

So far we have discussed about the electronic structures of radicals in which we explained the thermodynamic stability of the radicals through BDE, spin density, ESP, SOMO, NBO analysis and NICS calculations. In order to understand the reactivity and the kinetic stability of all radicals we have performed the (i) isomerisation pathways (1,2 and 1,3 H-shift). (ii) C-H bond cleavage of the radicals to form a biradicals which we are going to discuss in detail. (iii) Two more possible approaches that we performed are ring opening channels like unimolecular and concerted decomposition channels. Even after a lot of efforts, we could not obtain the concerted decomposition of the radical at higher level of theory.

2.9.1 1,2-H Shift

Interconversion barrier for the isomeric radicals of 2-, 3- and 4-hydroxy pyridine have been carried at (U)B3LYP/cc-pVTZ level of theory and the energy gap corresponding to the transition state is shown in the figure 2.10. The 3 α has one possibility, and in 3-hydroxy pyridyl radicals, we have 2 possibilities (i.e. from 2 β' to 2 γ or vice versa and 2 α' to 2 β'). The barrier for the transition of 3 α to 3 β is 68.3 (69.4) kcal/mol depending upon the level of

theory and basis set. Similarly, for 2- and 3-hydroxy pyridyl radicals, the energy of activation barrier ranges from 60.0 kcal/mol to 72.0 kcal/mol. The inter conversion of these radicals is kinetically less favourable as the energy barrier is high.

Table 2.12: Isomerization channels of dehydro-2-, 3-, 4-hydroxypyridyl radicals through 1,2-H shift in kcal/mol (Bold= (U)B3LYP/cc-pVTZ; Italics= (U)M062x/cc-pVTZ)

1,2 H-Shift	Reactant	TS	Product
3α to 3β	0.0	68.3	6.7
	<i>0.0</i>	<i>69.4</i>	<i>7.0</i>
2β' to 2γ	0.0	61.9	1.3
	<i>0.0</i>	<i>63.0</i>	<i>2.0</i>
2α' to 2β'	0.0	71.7	4.5
	<i>0.0</i>	<i>72.7</i>	<i>4.6</i>
1γ to 1β	0.0	62.7	2.3
	<i>0.0</i>	<i>64.5</i>	<i>3.2</i>
1γ to 1β'	0.0	64.7	2.5
	<i>0.0</i>	<i>66.4</i>	<i>2.9</i>
1α' to 1β'	0.0	71.0	6.9
	<i>0.0</i>	<i>72.0</i>	<i>6.6</i>

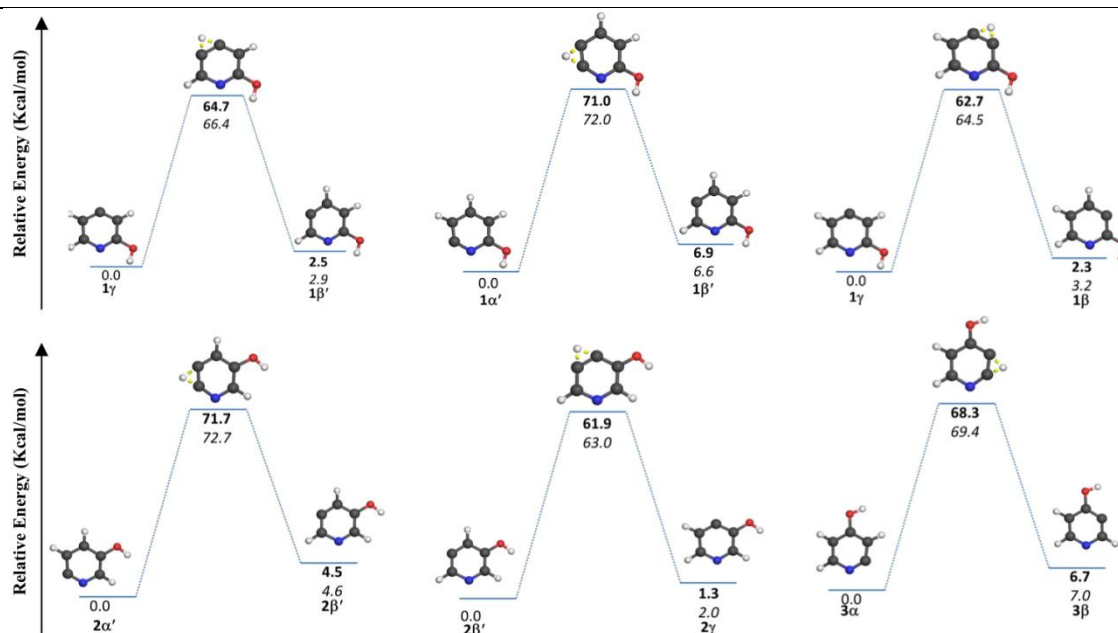


Figure 2.9: Isomerization channels of dehydro-2-, 3-, 4-hydroxypyridyl radicals through 1,2-H shift in kcal/mol (Bold= (U)B3LYP/cc-pVTZ; Italics= (U)M062x/cc-pVTZ)

2.9.2 1, 3-H Shift

1, 3-H shift have been performed to investigate the energy barrier for the interconversion between the *O*-centered and closest *C*-centered radicals. The idea behind doing this is to claim for the higher kinetic stability of the *O*-centered radicals as compared to its possible *C*-centered radical. The transition state barrier for the interconversion have been carried out at (U)B3LYP/cc-pVTZ and (U)M062X/cc-pVTZ levels of theory. **30** and **10** radicals had one possibility for the interconversion into isomeric carbon centered radicals. On the other hand, **20** had two possibilities (i.e. **20** to **2α** and **20** to **2γ**). The energy barrier corresponding to all the transition states ranged from 61.0 to 71.0 kcal/mol. Similar to the 1,2 H-shift, the transition pathways for 1,3 H-shift were found to be kinetically less favorable due to the higher activation energy barrier.

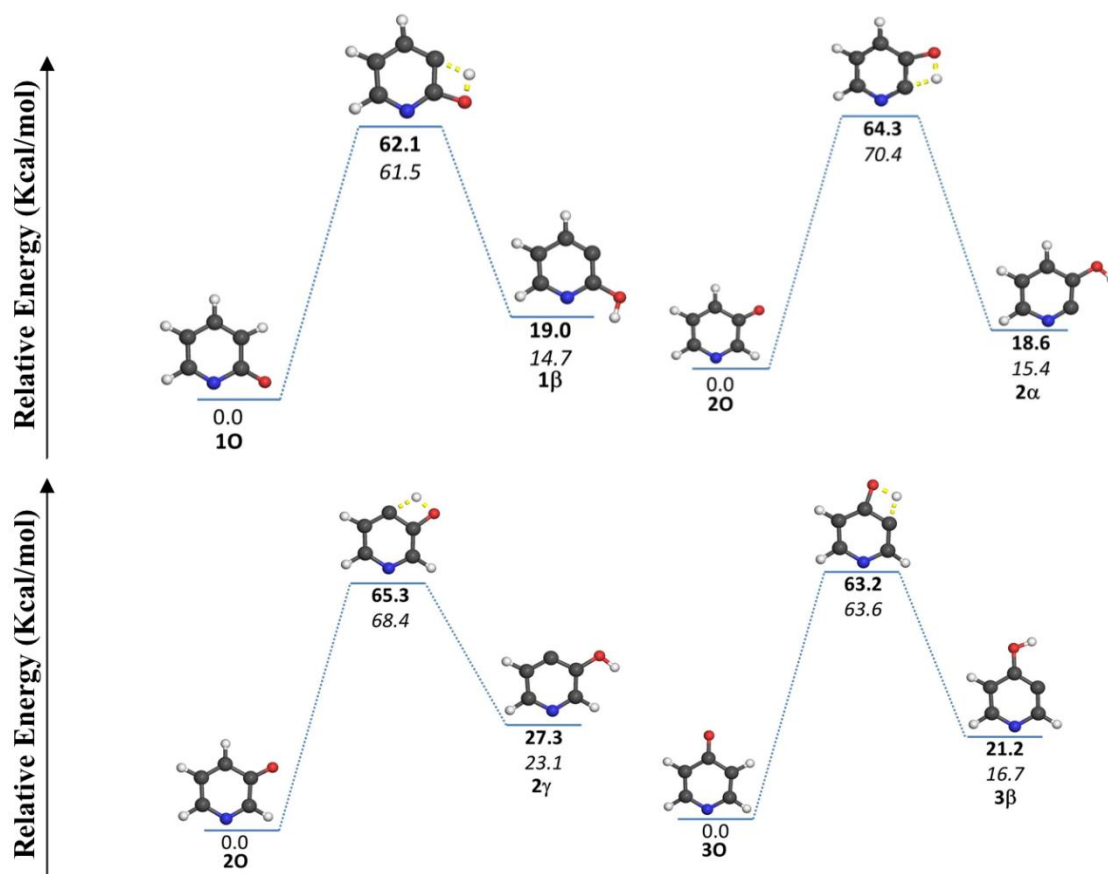


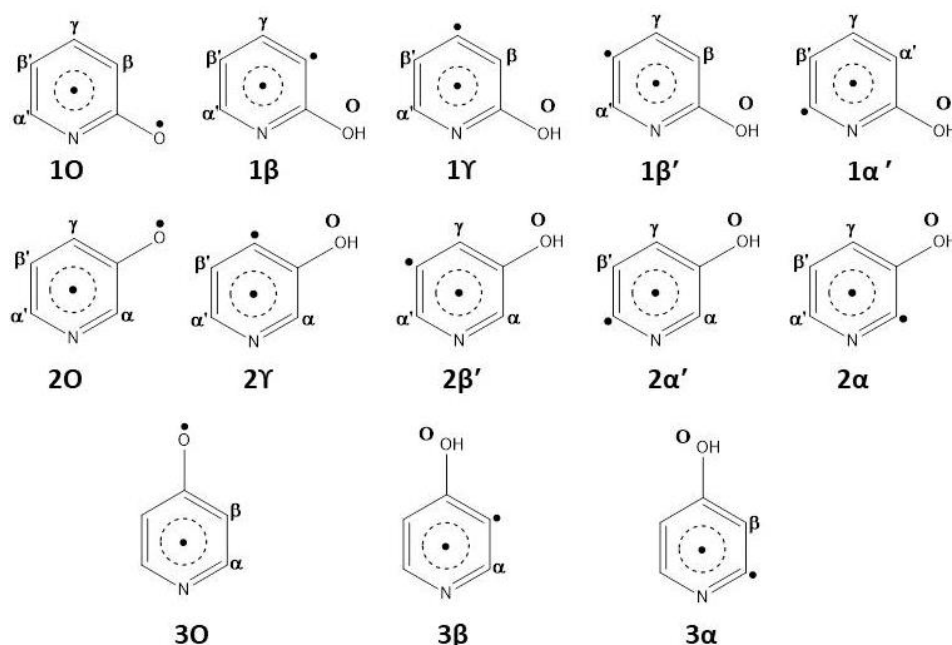
Figure 2.10: : Isomerization channels of dehydro-2-, 3-, 4-hydroxypyridyl radicals through 1,3-H shift in kcal/mol (Bold=(U)B3LYP/cc-pVTZ; Italics=(U)M062x/cc-pVTZ).

Table 2.13: Isomerization channels of dehydro-2-, 3-, 4-hydroxypyridyl radicals through 1,3-H shift in kcal/mol (Bold= (U)B3LYP/cc-pVTZ; Italics= (U)M062x/cc-pVTZ).

1,3 H-Shift	Reactant	TS	Product
3O to 3β	0.0	63.2	21.2
	<i>0.0</i>	<i>63.6</i>	<i>16.7</i>
2O to 2γ	0.0	65.3	27.3
	<i>0.0</i>	<i>68.4</i>	<i>23.1</i>
2O to 2α	0.0	64.3	18.6
	<i>0.0</i>	<i>70.4</i>	<i>15.4</i>
1O to 1β	0.0	62.1	19.0
	<i>0.0</i>	<i>61.5</i>	<i>14.7</i>

2.10 Biradicals

The C-H bond dissociation of the target radicals led to the formation of biradical and hydrogen atom. The sole purpose of biradical generation is to investigate the stable ground state of the biradicals. In this regard, we carried out the energy optimisations of the singlet and triplet ground states of the biradicals and also estimated the bond dissociation energies of the biradicals. The various possible biradicals have been shown in Scheme 2.3.



Scheme 2.3: Target didehydro-2-, 3-, 4-hydroxypyridine biradicals.

2.10.1 Singlet-Triplet Energy Gap of Biradicals

The various possible singlet and triplet biradicals have been computed at (U)B3LYP/cc-pVTZ level of theory. During our investigation, we observed most of the biradicals had their ground state as singlet except $10\beta'$, $20\alpha'$, $3\alpha\alpha'$, $2\alpha'\alpha$, $1\beta'O$, $2\alpha'O$ and $2\alpha\alpha'$. The singlet-triplet energy separation has been tabulated in table 2.14. Interestingly, we observed the increment in the singlet-triplet energy gap with the increase in spatial separation between the radical centers.

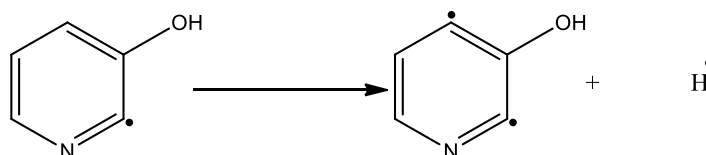
Table 2.14 Singlet-triplet energy separation for all the possible singlet/triplet biradicals at (U)B3LYP/cc-pVTZ level of theory.

Species	Absolute energy (Hartrees)	S-T gap (kcal/mol)	Species	Absolute energy (Hartrees)	S-T gap (kcal/mol)	Species	Absolute energy (Hartrees)	S-T gap (kcal/mol)
10β	-322.222904	0.0	20γ	-322.302301	-50.8	30β	-322.302295	-55.2
	-322.222904			-322.221395			-322.214279	
10γ	-322.280582	-35.5	$20\beta'$	-322.227293	-2.6	30α	-322.251151	-16.9
	-322.224009			-322.223118			-322.224155	
$10\beta'$	-322.198849	15.2	$20\alpha'$	-322.220026	6.9	$3\beta O$	-322.302294	-55.2
	-322.223096			-322.231034			-322.214279	
$10\alpha'$	-322.300876	-39.8	20α	-322.247440	-9.4	$3\beta\beta'$	-322.204849	-17.5
	-322.237495			-322.232398			-322.177035	
$1\beta\gamma$	-322.234599	-35.5	$2\gamma\beta'$	-322.221898	-37.4	$3\beta\alpha'$	-322.194052	-4.9
	-322.177978			-322.162323			-322.186283	
$1\beta\beta'$	-322.195880	-5.2	$2\gamma\alpha'$	-322.199602	-13.4	$3\beta\alpha$	-322.230083	-25.5
	-322.187609			-322.178319			-322.189426	
$1\beta\alpha'$	-322.199594	-3.7	$2\gamma\alpha'$	-322.213303	-20.9	$3\alpha O$	-322.251151	-16.9
	-322.193746			-322.180056			-322.224155	
$1\beta O$	-322.301264	-49.2	$2\gamma O$	-322.302294	-50.8	$3\alpha\beta'$	-322.188038	-2.5
	-322.222904			-322.221393			-322.184122	
$1\gamma\beta'$	-322.227880	-29.8	$2\beta'\alpha'$	-322.209776	-15.5	$3\alpha\alpha'$	-322.192976	3.9
	-322.180317			-322.185094			-322.199141	
$1\gamma\alpha'$	-322.221954	-16.6	$2\beta'\alpha$	-322.191854	-3.9	$3\alpha\beta$	-322.230083	-25.5
	-322.195550			-322.185644			-322.189426	

Species	Absolute energy (Hartrees)	S-T gap (kcal/mol)	Species	Absolute energy (Hartrees)	S-T gap (kcal/mol)
1 γ O	-322.280584	-35.5	2 β' O	-322.227293	-2.6
	-322.224009			-322.223118	
1 γ β	-322.234599	-35.5	2 $\beta'\gamma$	-322.221898	-37.4
	-322.177978			-322.162322	
1 $\beta'\gamma'$	-322.224293	-18.1	2 $\alpha'\alpha$	-322.176302	11.7
	-322.195524			-322.194870	
1 β' O	-322.198849	15.2	2 $\alpha'O$	-322.220025	6.9
	-322.223096			-322.231034	
1 $\beta'\beta$	-322.195880	-5.2	2 $\alpha'\gamma$	-322.199602	-13.4
	-322.187609			-322.178319	
1 $\beta'\gamma$	-322.227880	-29.8	2 $\alpha'\beta'$	-322.209776	-15.5
	-322.180317			-322.185094	
1 $\alpha'O$	-322.300876	-39.8	2 α O	-322.247442	-9.4
	-322.237495			-322.232398	
1 $\alpha'\beta$	-322.199594	-3.7	2 $\alpha\gamma$	-322.213303	-20.9
	-322.193746			-322.180056	
1 $\alpha'\gamma$	-322.221954	-16.6	2 $\alpha\beta'$	-322.191854	-3.9
	-322.195550			-322.185644	
1 $\alpha'\beta'$	-322.224293	-18.1	2 $\alpha\alpha'$	-322.176302	11.7
	-322.195524			-322.194870	

2.10.2 Second BDE

The second bond dissociation energy calculation has been performed for the formation of biradicals. The schematic picture of the second bond dissociation of the parent molecule is shown in Scheme 2.4 and the values for first BDE's are tabulated in Table 2.15, 2.16, 2.17 at (U)B3LYP/cc-pVTZ level of theory.



Scheme 2.4: Second bond dissociation energy leading to the formation of singlet/triplet biradicals.

Table 2.15: Second bond dissociation energy for all the possible singlet/triplet biradicals at (U)B3LYP/cc-pVTZ level of theory.

Reactant	Product	First BDE ΔH (kcal/mol)
1O	1O β + H \bullet	110.1
		110.1
	1O γ + H \bullet	74.9
		109.4
	1O β' + H \bullet	125.2
	110.0	
	1O α' + H \bullet	62.1
		101.0
1 β	1 $\beta\gamma$ + H \bullet	83.8
		119.3
	1 $\beta\beta'$ + H \bullet	108.4
		113.2
	1 $\beta\alpha'$ + H \bullet	105.8
	109.4	
	1 βO + H \bullet	42.0
		91.1
1 γ	1 $\gamma\beta'$ + H \bullet	90.3
		120.1
	1 $\gamma\alpha'$ + H \bullet	94.0
		110.5
	1 γO + H \bullet	58.2
	92.7	
	1 $\gamma\beta$ + H \bullet	86.0
		121.6
1 β'	1 $\beta'\gamma'$ + H \bullet	90.0
		108.0
	1 $\beta'O$ + H \bullet	105.9
		90.7
	1 $\beta'\beta$ + H \bullet	108.1
	113.0	
	1 $\beta'\gamma$ + H \bullet	87.8
		117.6
1 α'	1 $\alpha'O$ + H \bullet	49.7
		88.6
	1 $\alpha'\beta$ + H \bullet	112.4
		116.0
	1 $\alpha'\gamma$ + H \bullet	98.4
	114.9	
	1 $\alpha'\beta'$ + H \bullet	96.9
		114.9

Table 2.16: Second bond dissociation energy for all the possible singlet/triplet biradicals at (U)B3LYP/cc-pVTZ level of theory.

Reactant	Product	First BDE ΔH (kcal/mol)
2O	2O γ + H \bullet	59.8
		110.5
	2O β' + H \bullet	106.9
		109.4
	2O α' + H \bullet	111.3
	104.4	
	2O α + H \bullet	94.2
		103.6
2 γ	2 $\gamma\beta'$ + H \bullet	82.8
		120.3
	2 $\gamma\alpha'$ + H \bullet	96.9
		110.2
	2 $\gamma\alpha'$ + H \bullet	88.2
	86.4	
	2 γ O + H \bullet	32.4
		83.0
2 β'	2 $\beta'\alpha'$ + H \bullet	91.8
		107.2
	2 $\beta'\alpha$ + H \bullet	103.1
		106.9
	2 β' O + H \bullet	80.8
	83.3	
	2 $\beta'\gamma$ + H \bullet	84.1
		121.6
2 α'	2 $\alpha'\alpha$ + H \bullet	117.6
		105.6
	2 α' O + H \bullet	89.7
		82.8
	2 $\alpha'\gamma$ + H \bullet	102.7
	116.0	
	2 $\alpha'\beta'$ + H \bullet	96.3
		111.8
2 α	2 α O + H \bullet	75.6
		84.9
	2 $\alpha\gamma$ + H \bullet	97.0
		117.9
	2 $\alpha\beta'$ + H \bullet	110.5
	114.4	
	2 $\alpha\alpha'$ + H \bullet	120.5
		108.5

Table 2.17: Second bond dissociation energy for all the possible singlet/triplet biradicals at (U)B3LYP/cc-pVTZ level of theory.

Reactant	Product	First BDE ΔH (kcal/mol)
3O	3O β + H \cdot	56.5
		111.6
	3O α + H \cdot	88.7
		105.4
3 β	3 β O + H \cdot	35.2
		90.3
	3 $\beta\beta'$ + H \cdot	96.4
		113.7
	3 $\beta\alpha'$ + H \cdot	103.2
		108.0
3 α	3 $\beta\alpha$ + H \cdot	80.4
		106.0
	3 α O + H \cdot	74.1
		68.3
	3 $\alpha\beta'$ + H \cdot	113.7
		116.0
3 α	3 $\alpha\alpha'$ + H \cdot	110.5
		106.6
	3 $\alpha\beta$ + H \cdot	87.1
		112.7

2.11 Matrix Isolation

2.11.1 Deposition of 2-iodo-3-hydroxypyridine

The precursor, 2-iodo-3-hydroxypyridine (**IHP**) has been deposited along with excess amount of argon at 4 K. The spectral features were compared with the calculated spectra of the precursor molecule at B3LYP/DGTZVP level of theory. The spectra showed characteristic peaks at 3485.0 cm⁻¹ corresponding to OH stretching frequency and peaks at 1423.5 cm⁻¹ appeared as a most intense signal. Some of the signals were found to have splitting or change in intensity as compared to the calculated spectra, which may be due to the site effects of matrix. The deposited spectrum was in good agreement with the calculated spectrum within the limit of experimental shifts.

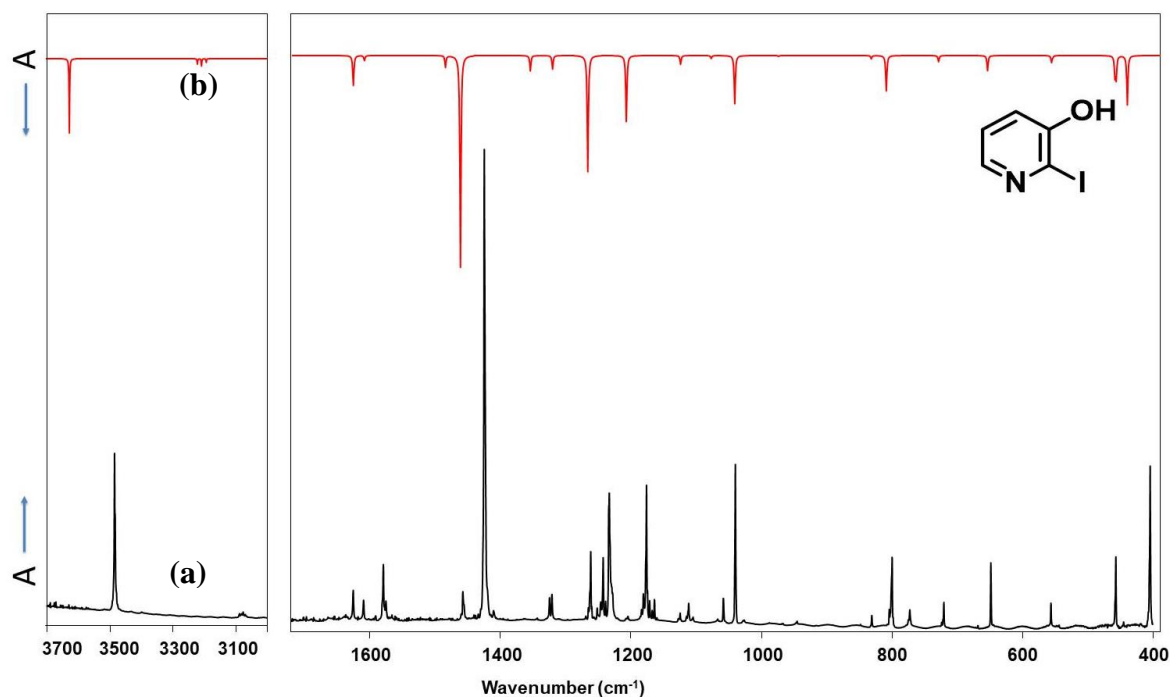


Figure 2.11: (a) Deposition spectrum of 2-iodo-3-hydroxypyridine (**IHP**) (Ar, 4 K, 1 hr, 200 °C); (b) Calculated spectrum of (**IHP**) (B3LYP/DGTZVP, unscaled).

2.11.2 Formation of 2-Dehydro-3-hydroxypyridine Radical

The deposited spectra was then irradiated with a low pressure mercury lamp ($\lambda=254$ nm) for 20 minutes. The spectra obtained showed bleaching of the precursor signals and new peaks appeared. One of the potential photochemical pathway is the radical formation by the homolysis of C-I bond at excited state. The matrix containing the photoproducts and the unreacted precursor was then further irradiated at 365 nm for 30 minutes. We observed that the precursor signals started rising accompanied by bleaching of some of the new signals that were formed during the irradiation at 254 nm. This indicates that the recombination of iodine with the dehydro-3-hydroxypyridine radical leading to the formation the precursor. Based on this evidence, we confirmed the formation of the radical and tentatively assigned the signals (3612.5, 1401.0, 1202.5, 1314.5 and 786.0) to it. Indeed, there are two possible radical isomers namely, *syn* and *anti*-forms. By comparing the calculated spectra of both the isomers, we observed that, the spectral features were matching with the *syn*-dehydro-3-hydroxy radical (*syn*)-3.

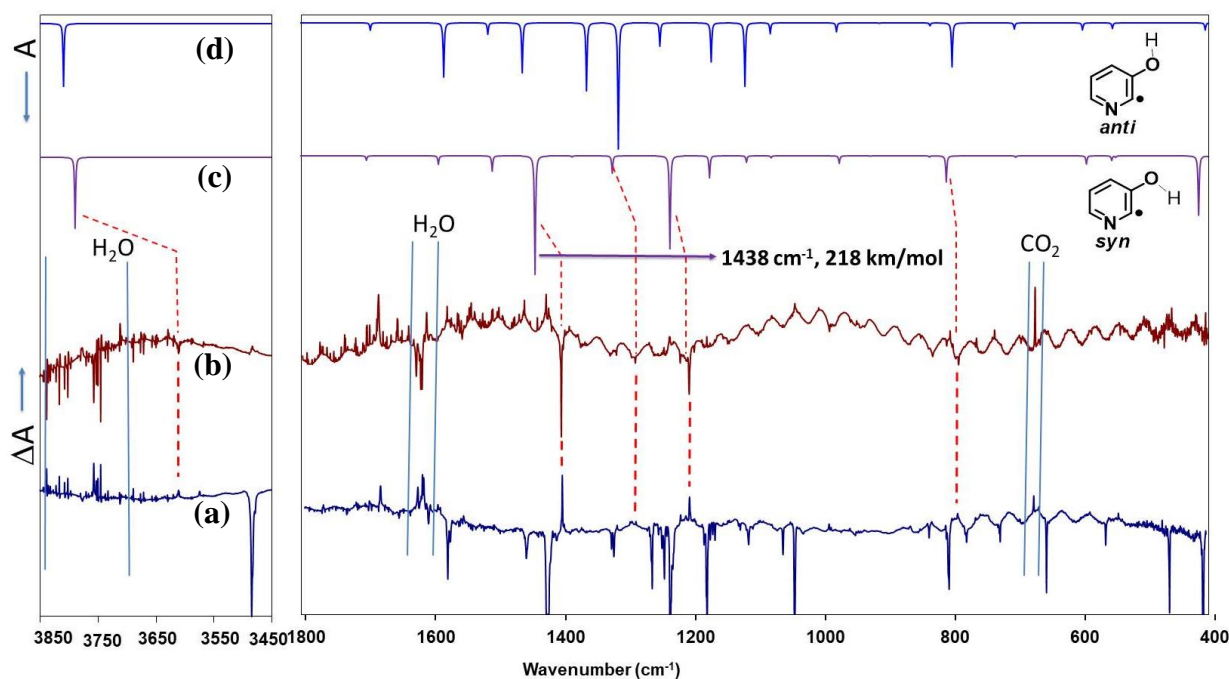


Figure 2.12: Photochemistry of 2-iodo-3-hydroxypyridine (**IHP**) in argon matrix (4 K, 400-1800 cm^{-1} region); The upward directing signals implies the formation of new species whereas downward directing signals signifies the disappearance of the precursor upon irradiation. **(a)** Difference spectrum after irradiation at 254 nm (75 min); **(b)** Difference spectrum after irradiation at 365 nm (75 min, the sequence was followed 254 nm irradiation); Calculated spectrum at ((U)B3LYP/cc-pVTZ, unscaled) of **(c)** *syn*- dehydro-3-hydroxypyridine and **(d)** *anti*- dehydro-3-hydroxypyridine

2.11.3 Formation of Ketene and Carbene

Along with radical signal there were other signals, which emerged after irradiation at 254 nm. One prominent signal with split band was observed around 2128.5 and 2133.5 cm^{-1} , and a sharp peak around 2142.0 cm^{-1} , which started appearing after shorter irradiation of about 20 minutes. Upon prolonged irradiation for about 5 hours, it was observed that the sharp peak at 2142.0 cm^{-1} increased prominently, but the split signals got almost bleached. The signal at 2142.0 cm^{-1} has been tentatively assigned to CO based on the earlier reports, and the split signals was tentatively assigned to C=C=O stretching of a ketene (2H-pyrrol-2-ylidene)methanone, which was further confirmed by calculated spectra.

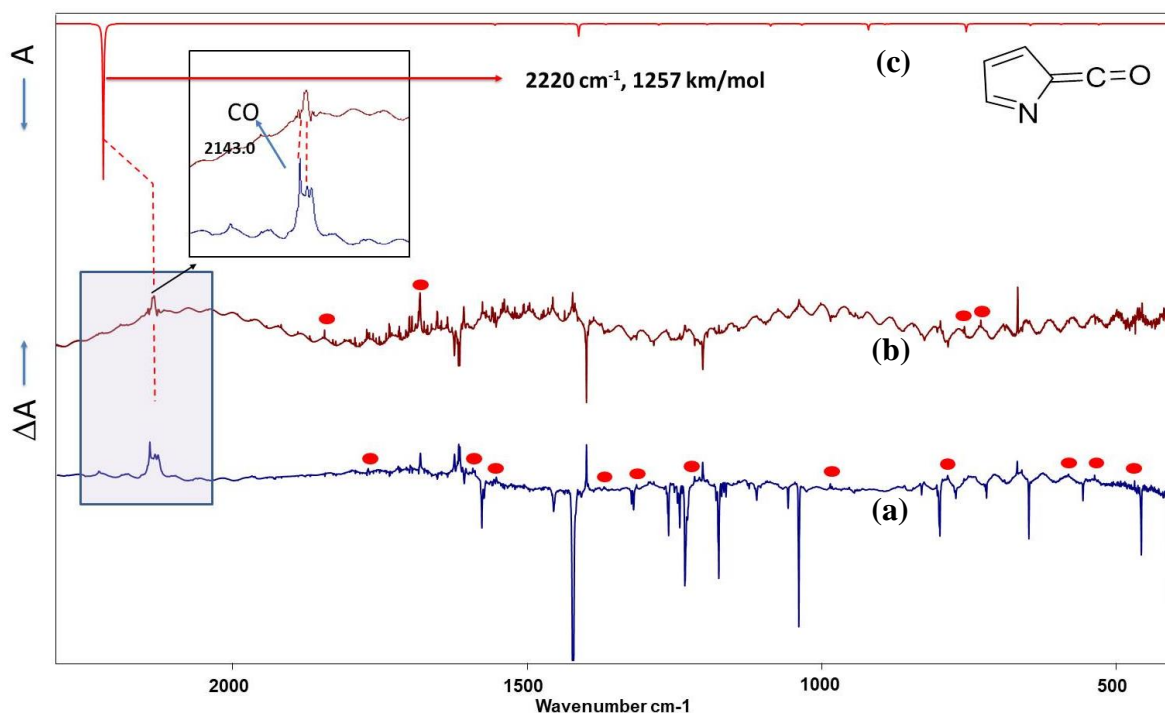


Figure 2.13: Photochemistry of 2-iodo-3-hydroxypyridine (**IHP**) in argon matrix (4 K, 400-1800 cm^{-1} region); The upward directing signals implies the formation of new species whereas downward directing signals signifies the disappearance of the precursor upon irradiation. **(a)** Difference spectrum after irradiation at 254 nm (75 min); **(b)** Difference spectrum after irradiation at 365 nm (75 min, the sequence was followed 254 nm irradiation); Calculated spectrum at ((U)B3LYP/cc-pVTZ, unscaled) of **(c)** (2H-pyrrol-2-ylidene)methanone. (Red circles: Unassigned peaks)

The C=C=O stretching in ketene has a very high intensity, so other characteristic signals could not be identified as the intensity of the experimentally observed C=C=O stretching itself is low. When the photoproducts were irradiated at 365 nm, it was observed that the signal at 2142.0 cm^{-1} dropped, and the ketene signal intensity started re-emerging. It suggests that prolonged irradiation at 254 nm causes the release of CO from the ketene to form a possible *N*-heterocyclic carbene, and on irradiation at 365 nm, CO recombines with carbene to form back the ketene. Based on the computed IR data, the signal intensity ratio between ketene and carbene was found to be about 10:1. Therefore, the characteristic peaks of carbene as such are not visible. At this juncture, the only proof of carbene formation is the CO elimination and recombination after 254 nm and 365nm, respectively.

2.11.4 Formation of Other Photoproducts

Apart from the ketene, carbene and radical, there are several other signals, which are not assigned yet. The signals could be possibly due to other photoproducts, and the analysis is underway. Some of the potential photoproducts include 7-oxa-2-azabicyclo[4.1.0]hepta-1,3,5-triene; 6-dehydro-pyridine-3(6H)-one; 6-Iodopyridine-3(6H)-one; didehydro pyridine-3-hydroxy biradical; NHC-carbene

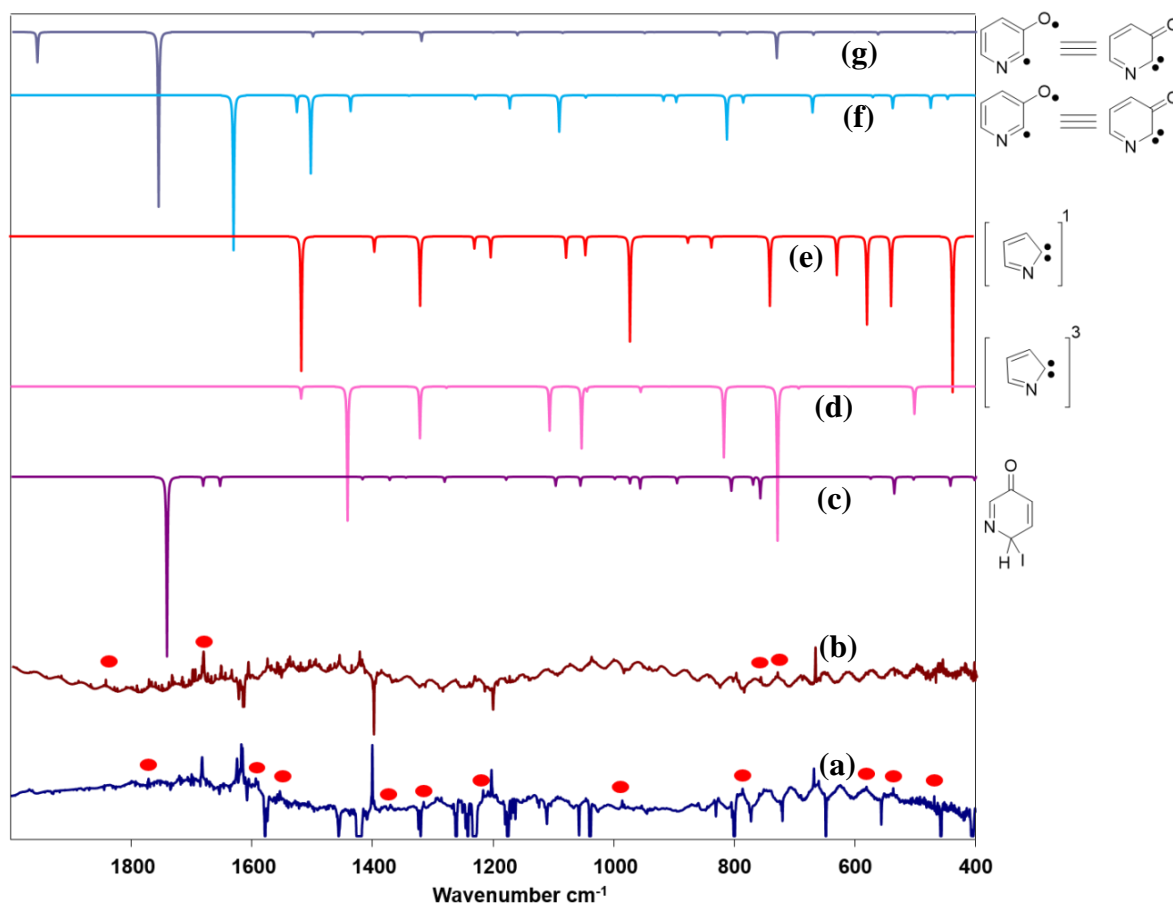


Figure 2.14: Photochemistry of 2-iodo-3-hydroxypyridine (**IHP**) in argon matrix (4 K, 400-1800 cm⁻¹ region); The upward directing signals implies the formation of new species whereas downward directing signals signifies the disappearance of the precursor upon irradiation. **(a)** Difference spectrum after irradiation at 254 nm (75 min); **(b)** Difference spectrum after irradiation at 365 nm (75 min, the sequence was followed 254 nm irradiation); Calculated spectrum at ((U)B3LYP/cc-pVTZ, unscaled) of **(c)** 6-Iodopyridine-3(6H)-one; **(d)** N-heterocyclic carbene (triplet); **(e)** N-heterocyclic carbene (singlet); **(f,g)** didehydro pyridine-3-hydroxybiradical. (Red circles: Unassigned peaks)

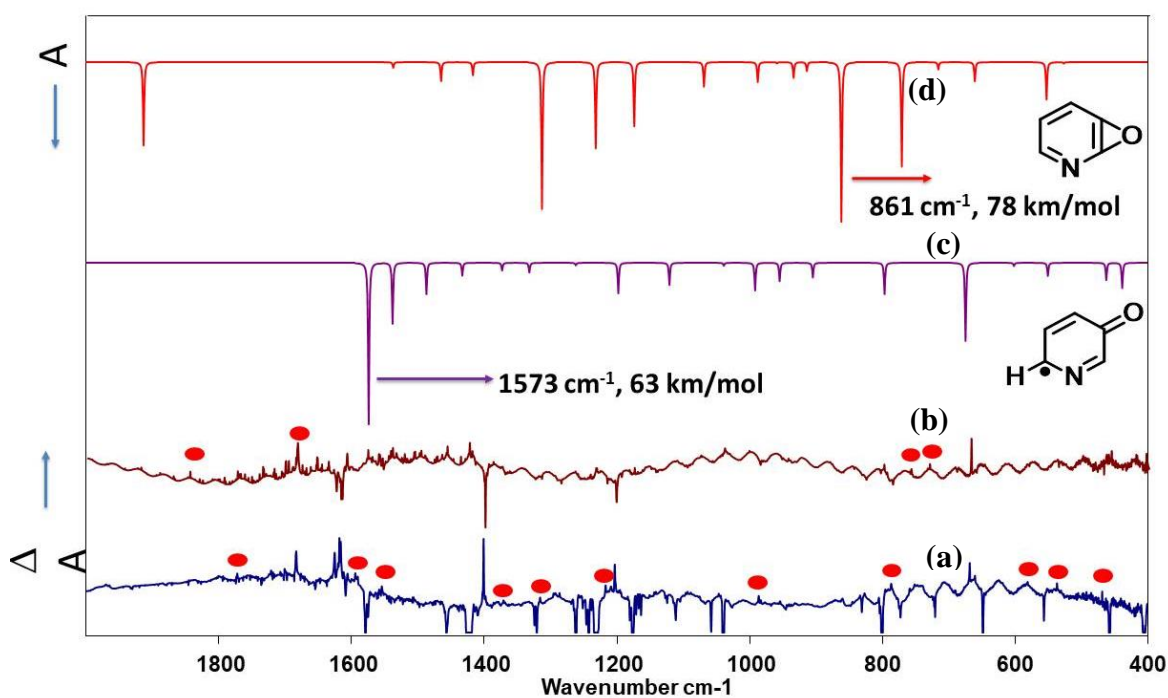


Figure 2.15: Photochemistry of 2-iodo-3-hydroxypyridine (**IHP**) in argon matrix (4 K, 400-1800 cm⁻¹ region); The upward directing signals implies the formation of new species whereas downward directing signals signifies the disappearance of the precursor upon irradiation. **(a)** Difference spectrum after irradiation at 254 nm (75 min); **(b)** Difference spectrum after irradiation at 365 nm (75 min, the sequence was followed 254 nm irradiation); Calculated spectrum at ((U)B3LYP/cc-pVTZ, unscaled) of **(c)** 6-dehydro-pyridine-3(6H)-one; and **(d)** 7-oxa-2-azabicyclo[4.1.0]hepta-1,3,5-triene. (Red circles: Unassigned peaks)

2.12 Computational Investigations on the Pathways Leading to Carbene

Based on the observation of a ketene in our experimental part, we mainly considered the unimolecular decomposition pathway leading to ring contraction. In this regard, we considered two possible pathways. One of which is through the formation of an epoxide (energy barrier of 44.2 kcal/mol), however, attempts on further ring opening channels were not successful. An alternative pathway was the O-H bond cleavage leading to the formation of a biradical. The ring contraction of the biradical *via* C-C bond cleavage (energy barrier of 9.3 kcal/mol) leads to the ketene. The ketene formed was found to be more stable than the biradical by 33.8 kcal/mol, and hence the exothermic reaction is expected to be more facile. Further elimination of carbon monoxide leads to the formation of primitive *N*-heterocyclic

carbene (NHC) with a kinetically favorable energy barrier. The intermediates formed from these transition states were thermodynamically less stable as compared to the reactants. Although, the intermediate formed through the C-C bond cleavage, which resulted in the formation of ketene had lesser energy compared to the reactant. In summary, the C-C bond cleavage leading to the ketene formation was thermodynamically the most favorable pathway whereas epoxide formation was the least favorable one.

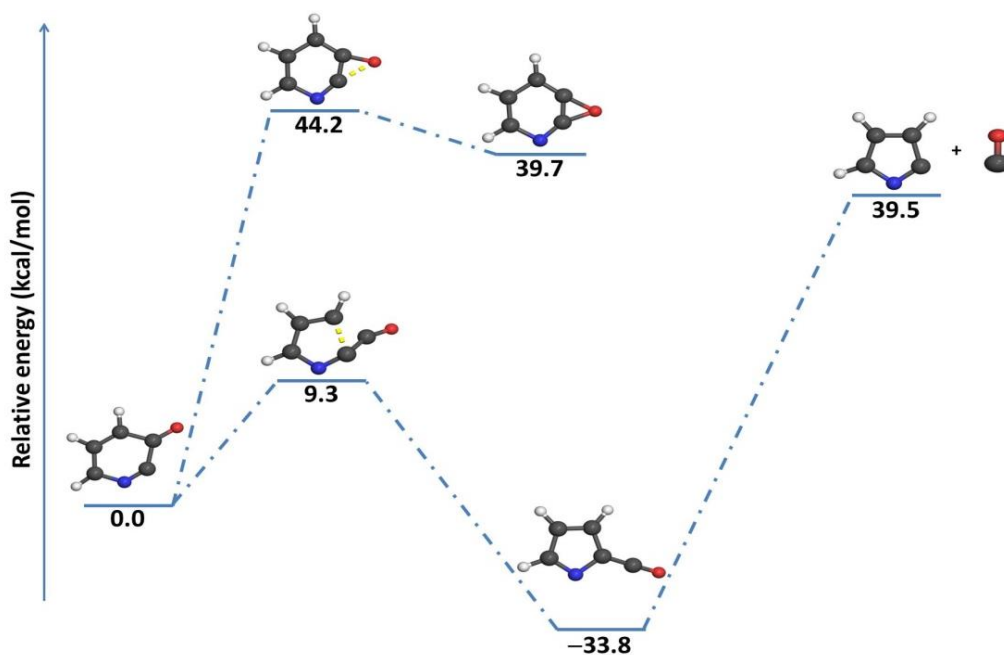


Figure 2.16: Ring-opening pathway of the *2-dehydro-3-hydroxy pyridyl radical* (2α) at (U)B3LYP/cc-pVTZ level of theory.

Chapter 3: Summary and Outlook

3.1 Summary

As discussed before the through space or through bond interactions are gaining valuable insights considering the stability of heterocyclic radicals are crucial to many biochemical processes and metabolism. In our group's previous study on dehydro-pyridyl radicals, the stabilizing interaction between the lone pair of nitrogen and the respective radicals have been understood. Now in our current molecules of interest, there is a possibility of competition between the lone pair of oxygen and the lone pair of nitrogen in stabilising/destabilizing the radical.

The electronic structure and stability patterns of dehydro-2-, 3-, 4-hydroxy pyridyl radical isomers have been investigated using quantum chemical calculations. The analysis of geometrical parameters gives insights about the changes in the structural aspects as an effect of radical formation, which also gives some hints about the interaction of radical with atomic centers. The stability order of all the radical isomers were determined and compared among each molecule. The spin density and electrostatic potential diagram shows the distribution of electron density over the molecule, which in turn gives us an idea of the interaction of radical center. The SOMO and MOs gives us an idea of the type of interaction at the radical center with rest of the molecule. A clear quantitative picture has been obtained using the natural bond analysis.

After performing and analysing many calculations, it was observed that nitrogen lone pair is more dominating in stabilising the radical as compared to the oxygen lone pair. The reason maybe because the oxygen is more electronegative than the nitrogen so have less ability to stabilise the radical and also the nitrogen is present in the ring which makes it more selective for stabilizing the radical by through space or through bond interactions as compared to oxygen. Evidence for the above statement is the greater relative stabilization of *syn* isomer than *anti*, which may be attributed to the repulsion between the oxygen lone pair and the radical center.

Apart from the structural aspects of these radical isomers, the reactivity traits also been investigated for dehydropyridyl radical isomers. The isomerization channels studies of all the

radical isomers and the unimolecular decomposition studies of 2α gives us an idea about the kinetic stability of the radical isomers.

Furthermore, the electronic structural studies of didehydro-2-, 3-, 4-hydroxy pyridyl biradicals have also been carried out for understanding the radical-radical interactions. The calculations of the singlet-triplet energy gap been determined for better understanding of the ground state spin multiplicities.

Exploration of the structure and stability patterns of the radical isomers of dehydro-2-, 3-, 4-hydroxy pyridyl suggests that the radical isomer, which is having the radical center over the oxygen atom, is more stable than at carbon centered. The carbon centered radicals show energy values that are close to each other, as compared to the oxygen centered radical. The higher stability can be attributed to the delocalisation of radical with the π bonds of the ring. The results were confirmed after exploring the BDE, spin density, NBO and NICS calculations.

Besides the thermodynamic stability analysis, the kinetic stability of dehydro-2-, 3-, 4-hydroxy pyridyl radical isomers has also been examined by determining the isomerization channels like 1,2 H-Shift and 1,3 H-Shift.

The 2-dehydro-3-hydroxy pyridyl radical was investigated experimentally by matrix isolation infrared spectroscopy technique at 4 K. The iodo precursor was deposited and irradiated at 254 nm leading to the formation of the target radical. On prolonged irradiation, a ketene formation was observed along with the formation of CO. Subsequent irradiation at 365 nm led to decrease in CO signal intensity, and an increase in ketene signal intensities. On reversing the irradiation wavelength back to 254 nm, we observed the decrease in ketene signal and increase in CO intensity indicating the possibility of the presence of NHC carbene. Experiments are underway to further strengthen our initial results.

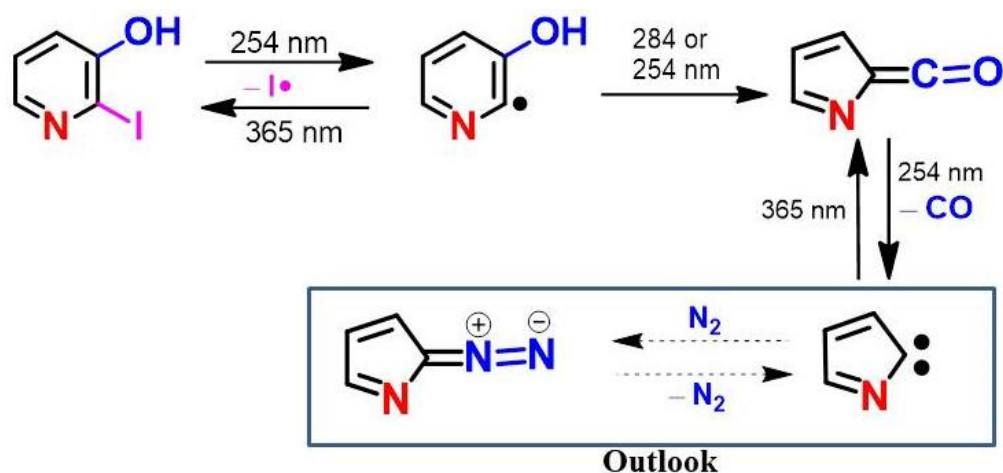


Figure 3.1: Summary and Outlook

3.2 Outlook

Based on our computational studies, the most significant result that we obtained was the delocalization of the radical electron in π -orbitals of oxygen-centered radical of dehydro-2-, 3-, 4-hydroxy pyridyl oxy radicals as compared to their respective hydroxy pyridyl radicals. The results were consistent with different levels of theory.

Oxygen centered biradical is an interesting candidate for the high spin system as it can be used in the generation of molecular magnets. In this regard, we need to explore the radical-radical interactions for the better understanding of the high spin ground state.

Apart from the computational studies we isolated the 2-dehydro-3-hydroxy pyridyl radical using matrix isolation infrared spectroscopy with argon matrix. Among the photochemical products of the radicals, one of the suspected photoproduct is likely to be N-heterocyclic carbene which needs to be confirmed with nitrogen matrix.

Chapter 4: Materials and Methods

4.1 General Methods

4.1.1 Computational Details

All the structures were optimized at (U)B3LYP and (U)M06-2X with different basis set using Gaussian 09 software package⁴⁰. Single-point energy calculations were performed at (U)CCSD(T) using (U)B3LYP/cc-pVTZ optimized geometries to obtain better precision in thermochemistry data. Vibrational frequencies calculations were done including the zero-point energy corrections. for the confirmation of minima. Apart from this, second-order perturbation energy values were calculated from natural bonding orbital (NBO) calculations using the G09/NBO package at (U)B3LYP/cc-pVTZ level of theory.

4.1.2 Experimental Details

The sample of 2-iodo-3-hydroxypyridine was commercially purchased from sigma Aldrich and was used without further purification. The sample was premixed with high purity argon gas (Sigma Aldrich, 99.9995% purity) along the vacuum line and was co-deposited on a KBr disc cooled at about 4 K by a three-stage closed cycle helium compressor. Preliminary experiments were carried out to standardise the deposition conditions for the precursor, 2-iodo-3-hydroxypyridine. The sample being of low vapour pressure the sample was sublimed at 200 °C using a BUCHI hot oven for about a 60 min. Spectra were recorded using BRUKER TENSOR II FT-IR spectrophotometer. All spectra were recorded with 0.5 cm⁻¹ resolution and number of accumulation was averaged to be 128 scans. A low pressure mercury lamp and convoy 365 nm UV torch lights were used for inducing photoreaction. DFT calculations were carried out in-order to get the IR spectral patterns of the precursor, products and intermediates.

4.2 Theoretical Insights and Computational Methods

4.2.1 History and Developments in Computational Chemistry

Computational chemistry is a viable tool in understanding the various mechanisms and concepts in different fields of chemistry. Computational chemistry started developing under the lights of theoretical chemistry and chemical physics. It basically uses its theorem and postulates for understanding the dynamics of the system, its thermochemistry and kinetics. Calculations of many molecular and atomic properties were possible after some developments in the field of quantum theory in 1920s, but the development of the Hartree-Fock equations in this field was the major breakthrough in the year 1930. Gaussian-type basis functions for simulating orbitals was introduced in the year 1950 and then in the following year Roothaan and his coworkers laid the foundations of computational chemistry by the development of the matrix version of HF method. It is Roothaan's equations which are used and are the backbone to several algorithms used in different computational suites used for *ab initio* calculations. Quantum mechanics thus developed a path that lead to the formation of computational Chemistry⁴¹.

Thomas and Fermi independently developed a theory using statistical mechanics that could relate the electron density on a system with the average energy of the system in the year 1927. The theory remained static for a few decades till the Hohenberg-Kohn Theorem came into picture. The Hohenberg-Kohn-Sham version of the theorem was another breakthrough in the field of computational chemistry. This theory used functional instead of the quantum mechanical wave function and was widely celebrated as the Density Functional Theory.

Density functional theory (DFT) is regarded to be a very accurate method for determining the electronic structure with a lesser computational cost. It uses an approximate Hamiltonian in terms of the electron density rather than using a wave function. In DFT calculations, the total energy is expressed in terms of the electron density. For the better computational results produced by DFT as well as for its wide applications, Walter Kohn was awarded the Nobel Prize in Chemistry for “his development of the density-functional theory”⁴².

Molecular properties such as structures, energies, frequencies, dipole moments and electron distribution can be obtained using such calculations. Computational chemistry has developed into an independent branch of chemical sciences due to the emergence of better technologies,

computational efficiency and algorithms. Hybrid theories which combine DFT and quantum mechanical methods are very popular and have been exploited for analyzing our system of interest.

4.2.2 Density Functional Theory (DFT)

DFT is one of the standard computational tools used in the field of academia and industry. DFT is one of the dominating quantum method in calculation of total energies and help in the prediction of the structure as well as the thermodynamic and kinetic stability of the molecules. These calculations also provide the finer details of the electronic structure of the system of interest.

Density Functional Theory (DFT) computes the property of system by means of electron density which is a function of $3N$ coordinates (i.e. x, y, z). The beauty of DFT lies in the fact that it does not use the wavefunction but it uses the square of wavefunction for the measurement of electron density. Thus electron density can be defined as the probability of finding N electrons in a system confined within a volume element. The advantage of density functional theory over other computational methods is that the electron density is a observable quantity and can be measured experimentally by X-ray diffraction. For an N electron system; electron density depends upon $3N$ variables (i.e. x, y, z) but it can also be dependent on $4N$ variable if we take spin of electrons into account.

In 1964, Hohenberg and Kohn came up with the fact that ground state properties are functionals of electron densities. The theorem of Hohenberg and Kohn is a proof of such a functional, but so far there is no method of constructing it. Unfortunately, we do not know the exact form of energy functional, thus one need to use an approximation dealing with kinetic energy and exchange correlations energies of the electrons comprised in a system. The approximation used is Thomas-Fermi term for kinetic energy and the Dirac term for the estimation of exchange energy. The combined functional containing both kinetic energy and exchange energy came to be known as Thomas-Fermi-Dirac energy.

The functional used in Thomas-Fermi method can be improved as they are not reliable for molecular systems. Thus the improvements on the Thomas-Fermi method lead to true density functional method. In this regard, density functional method is a boon from other methods which helps in computing energy through electron density alone in many particle systems.

Density functional theory can very well predict the chemical bonds in a molecule, which was one of the drawbacks of Thomas-Fermi theory.

For the better generalization of Density functional theory, Hohenberg and Kohn propose the following postulates: (1) every quantum mechanical property including the thermochemistry can be calculated from ground state density. (2) The ground state density can be calculated using the variational method involving only the electron density. The above two postulates can be generalized within Born-Oppenheimer approximation; the ground state of a system containing electrons is a result of the nuclei position. The choice of Hamiltonian has to be done in such a way that the kinetic energies of electrons and also the electron-electron interactions adjust themselves to the external nuclear potential. It is the external potential which is a variable term plays a dominating role in deciding the lowest energy of the system.

DFT being a function of electron density, the total energy of the system should be expressed in terms of electron density. In case of electron-electron interaction, consider $\rho(\mathbf{r})$ as a set of electrons in a vicinity of radius r and assume that each electron is interacting with the total electron density in that space. This particular interaction can be expressed using coulomb energy and the integration over the entire electron gives us the complete electron-electron interaction energy. The V_{ext} can also be expressed as the product of nuclear position and electron density over the space. The kinetic energy term has been expressed as a function of electron density by a formula derived by Thomas Fermi. Thus, DFT proves that each individual energy term can be expressed in terms of electron density and also confirms the Hohenberg-Kohn theorem which states that ground state energy can be obtained from electron density^{43,44}.

4.2.3 Basis Sets

Basis sets is a mathematical formulation of the linear combination of orbitals which are required to ensure the minimum energy of the molecule. The beginning of basis sets started with Slater Type Orbitals (STO/nG) where n is number of Gaussian type orbitals (GTO). The STO basis set was restricted only to the core electrons and therefore it cannot be used for many electron systems which were the major drawback of the STO for computational calculations⁴⁵. The shortcomings of STO were improved by the split-valence basis sets which had the distinguish ability between the core and valence electrons. For example, in 3-21 G,

the core electrons are made up of 3 gaussian type orbitals whereas each valence electron is comprised of 3 (2+1) gaussian orbitals⁴⁶.

The advancement in basis sets came up with the inclusion of diffused basis sets and the polarised basis sets. For example, 6-31 G(d,p) is a polarised basis set which adds an 'p' flavour to 's' orbital and 'd' flavour to 'p' orbital. Apart from this the diffused basis set (6-31++G (d,p)) increases the size of the 's' and 'p' orbitals in addition to their polarisability. Addition to the above discussed basis sets, cc-pVNZ where N=T, D,... (D=double-zeta, T=triple-Zeta...) are also used where "cc-p" stands for "correlation consistent polarisation" and the "V" indicates the "valence". The whole idea behind the advancement of the basis sets is to avoid nuclei-electron interaction in order to ensure the lowest possible energy of the molecule⁴⁷.

4.2.4 Bond Dissociation Energy (BDE)

The strength of a chemical bond can be estimated by calculating its bond dissociation energy. In principle, it is defined as the enthalpy change when a bond is ruptured in a chemical reaction. The difference between the enthalpy of products and reactants involved in the reaction gives the bond dissociation energy corresponding to the bond being ruptured. The BDE value also gives useful information regarding the feasibility of the reaction and also the thermodynamic stability of the molecule of interest. Thus it can be concluded that lower is the BDE value, greater will be the thermodynamic stability⁴⁸.

4.2.5 Natural Bond Orbital (NBO) Analysis

NBO analysis is basically used for transformation of a wavefunction into a localised form which corresponds to lone pair and bond element of the lewis structure. More precisely, NBOs are of two types: (1) lewis-type NBOs (which determines the localisation) (2) non lewis-type(which describes the delocalisation) The sole purpose of the analysis is to give the quantitative interactions between the bond pairs as well as the lone pair and bond pairs. In this regard these calculations are quite useful for the better understanding for the systems containing lone pairs and the radical. Apart from this, it also provides useful interaction energies for explaining the stability of H-bonded complexes by means of donor and acceptor orbitals used in the interplay^{49,50}.

4.3 Matrix Isolation Infrared Spectroscopy

4.3.1 Technique and Experimental Setup

The isolation and the characterization of reactive intermediates is a challenge for physical organic chemists all over the world due to high reactivity of intermediates. In principle, one can overcome this challenge by using ultrafast spectroscopy and matrix isolation spectroscopy. Matrix isolation is a technique used for spectroscopic characterization of reactive intermediates. In this technique, the guest molecules are trapped in rigid host materials. The choice of precursor of the molecule of interest has to be such that it contains a labile group so that it can be converted into the desired reactive species. In general, the precursor is deposited along with host gas (1:1000) onto a cold spectroscopic window. The host gases such as argon, neon and nitrogen are chosen since they are inert gases. The conversion of the precursor into the desired reactive species can be accomplished by photolysis and pyrolysis. Thus, in the process the reactive species are well isolated in the rigid host matrix. The host gases are taken in excess in order to avoid diffusion and intermolecular interactions.

The art of matrix isolation technique was developed by George Pimentel along with George Porter. The studies of the reactive intermediate can be achieved in two ways: (1) the detection after their immediate formation or (2) detection of the trapped molecule of interest after a certain period of time. Thus in this way, the former allows the kinetic study whereas the latter allows the electronic structural properties of the reactive intermediates.

4.3.2 Advantages of Matrix Isolation

Matrix isolation technique has several advantages over other techniques used for the detection of reactive intermediates. Firstly, the inert nature of the gases allows for temperature dependent studies as the gases due their unreactive nature does not involve in any interaction with the reactive species of interest. Secondly, the homo-nuclear diatomic gases used have their transparency in the IR and the UV-Visible range. The inert nature is quite useful in providing higher resolution to the spectra which allows the much easier study of the complex structure. Thirdly, the generation of reactive intermediates by thermolysis or photolysis, and their deposition onto the cold window at low temperatures ranging from 4 K-10 K suppresses any type of reactions within the matrix. Lastly, apart from detection of

reactive intermediates, it is also useful for the study of weak interactions like Vander waals complexes and other molecular conformations. Mechanisms involving hydrogen bonding and charge transfer can be also well understood by using this technique under low temperature matrices.

4.3.3 Limitations of Matrix Isolation

Interestingly, with so many advantages it has certain limitations. The first limitation is being the size of the precursor and also its volatility. The choice of the precursor has to be such that it is highly volatile and its size should be small enough for the vaporization and its immediate deposition onto the cold window. Secondly, it has restrictions on polar molecules as they have a tendency to aggregate which makes the isolation of the reactive intermediates difficult. Thirdly, there is a possibility of recombination even after the formation of reactive intermediate to give back the precursor due to the cage effect.

4.3.4 Photochemical Studies and Bimolecular Reactions under Matrix Conditions

The radical isolated in the matrix on irradiation with UV or visible light may result in either rearrangement or ring opening products which are of much interest to interstellar chemistry. There is also a high chance of O₂, CO, or CO₂ to diffuse rapidly if the matrix is annealed at a temperature of 30-50% of its melting point. For example, when argon matrix is annealed at 30-35 K these bimolecular reactions are often observed by spectroscopy. These bimolecular reactions can be avoided if the radical has been produced photochemically because under photochemical conditions, recombination of radical pair will lead to the precursor molecule. In principle, IR spectroscopy is useful for gathering vibrational and rotational information of the molecules but due to low temperature the rigidity of the matrix inhibits the rotational motion of the trapped molecules which results in fine spectra in contrast to its spectra in the gaseous phase.

4.3.5 Instrumental Setup

The main components of matrix isolation setup are Cryostat, Helium Compressor, Temperature Controller, Vacuum system and FTIR spectrometer.

4.3.5.1 Cryostat

Cryostat (RDK-408D2 from Sumitomo cryogenics) is used to get the cold temperature, which is required for the solidification of the inert gas. The gases like N₂, Ar, Ne, requires very low temperature to form matrices. The common cryogenic fluids like liquid N₂, liquid He, and liquid H₂ are used in cryostat to obtain low temperatures. The cold head is well fitted with a KBr window for IR studies and a quartz window for UV-Vis spectroscopic studies.

4.3.5.2 Helium Compressor

In our matrix isolation setup three-stage closed cycle helium compressor (Sumitomo Heavy industries Ltd.) is used to produce 4 K temperature, which is equipped with the cryostat. A water cooled helium gas compressor unit (F-70L from Sumitomo cryogenics) needs to be used in this regard to achieve the desired 4 K temperature. For achieving low temperature of the range 4 K, the cold head of the cryostat is connected with the compressor by means of two bellow hoses. The cooling mechanism at the cold head of the cryostat is governed by the principle of Joules Thomson cooling effect.

4.3.5.3 Temperature Controller

The optical window used at the cold head of cryostat is connected with a temperature controller (LakeShore model No. 336) along with a temperature sensor. This has the possibility to heat the window to desired temperature to perform annealing experiments, where the solid inert gases are allowed to soften such that the diffusion of the trapped species can be enabled.

4.3.5.4 Vacuum System

The matrix unit is comprised of two pumps namely (a) Oil rotary vane pump and (b) Diffusion pump. The purpose of the rotary pumps is to remove bulk of the air molecules which are initially at atmospheric pressure. The removal of high volume of air molecules lowers the pressure from 1 atm to 10⁻³ mbar. Once the sufficient vacuum around 10⁻³ mbar is setup, then the other pump i.e. diffusion pump can bring the pressure to 10⁻⁶ mbar. The attainment of 10⁻⁶ mbar is the required condition to start matrix isolation experiment.

4.3.5.5 FTIR Spectrometer

Fourier-transform infrared spectroscopy (FTIR) is a technique which is used to convert the raw data into the actual spectra. It is a technique which is widely used for the interpretation of infrared spectrum of solid, liquid and gaseous sample. It has an extra edge over other spectrometer as it measures intensity over much narrower range of wavelengths. A Bruker Tensor II FTIR spectrometer has been installed for recording the IR spectra.

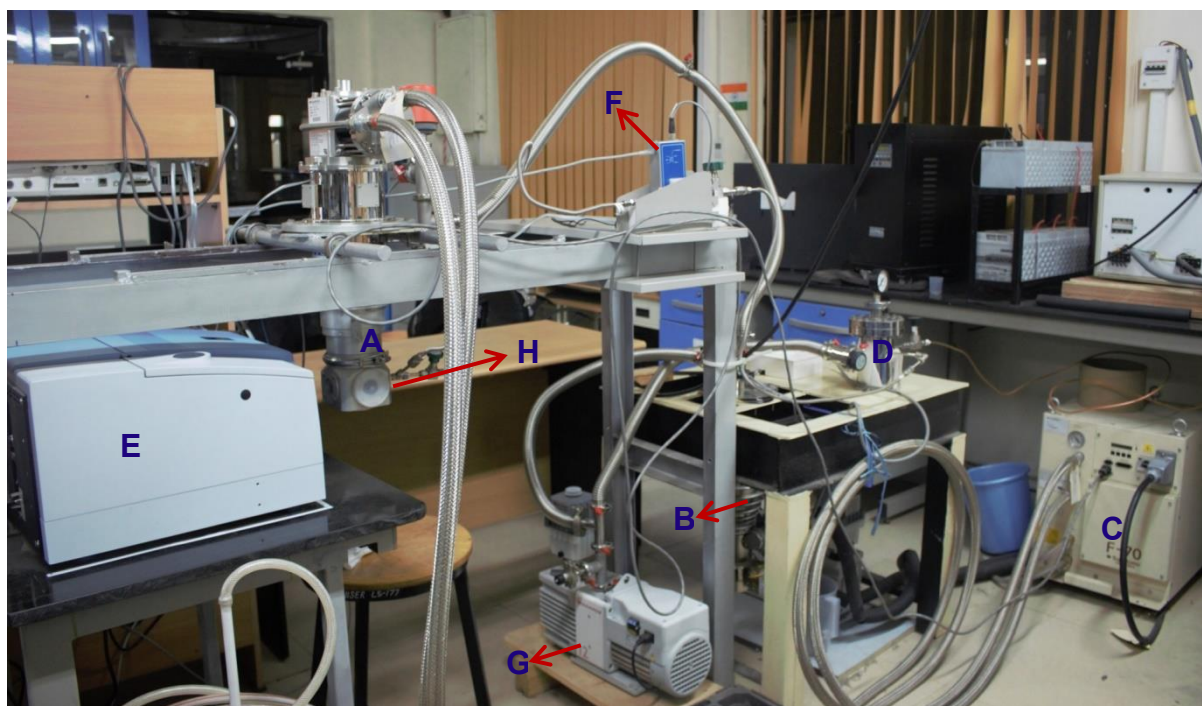


Figure 4.1: Matrix Isolation FT-IR setup at POC lab

A: Cryostat, **B:** Diffusion pump, **C:** Helium compressor, **D:** Mixing chamber for inert gases, **E:** IR spectrometer, **F:** Flow controller, **G:** Rotary vane pump, **H:** KBr window

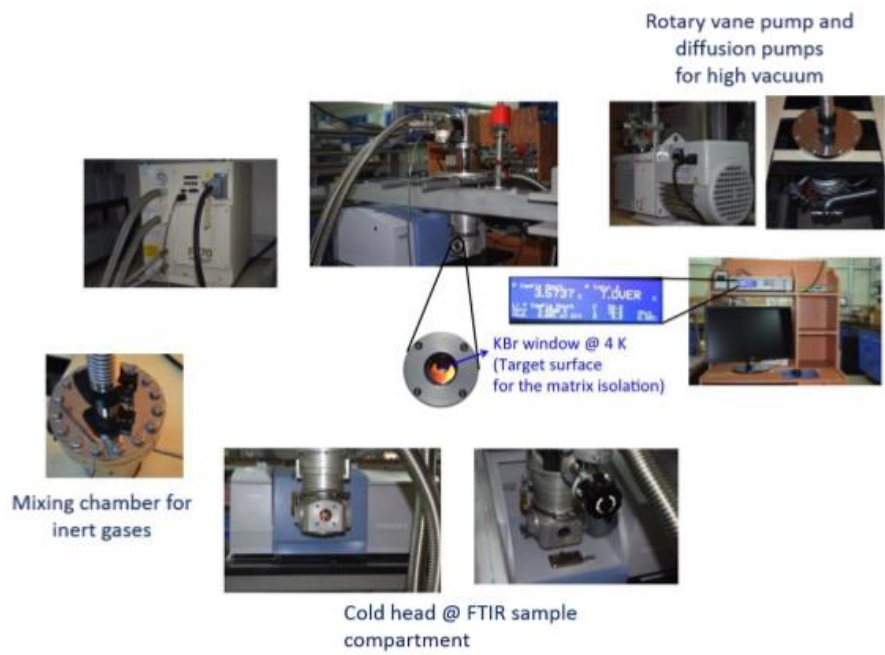


Figure 4.2: Different parts of the Matrix Isolation Setup

References

- (1) Gomberg, M. Organic Radicals. *Chem. Rev.* **1924**, *1* (1), 91–141.
- (2) Nakamura, T.; Takegami, A.; Abe, M. Generation and Intermolecular Trapping of 1,2-Diaza-4-Silacyclopentane-3,5-Diyls in the Denitrogenation of 2,3,5,6-Tetraaza-7-Silabicyclo[2.2.1]Hept-2-Ene: An Experimental and Computational Study. *J. Org. Chem.* **2010**, *75* (6), 1956–1960.
- (3) Moss, R. A.; Platz, M.; Jones, M. *Reactive Intermediate Chemistry*; Wiley-Interscience, 2004.
- (4) Matyjaszewski, K.; Xia, J. Atom Transfer Radical Polymerization. *Chem. Rev.* **2001**, *101* (9), 2921–2990.
- (5) Michelmore, A.; Whittle, J. D.; Bradley, J. W.; Short, R. D. Where Physics Meets Chemistry: Thin Film Deposition from Reactive Plasmas. *Front. Chem. Sci. Eng.* **2016**, *10* (4), 441–458.
- (6) Orlando, J. J.; Tyndall, G. S.; Wallington, T. J. The Atmospheric Chemistry of Alkoxy Radicals. *Chem. Rev.* **2003**, *103* (12), 4657–4690.
- (7) Gligorovski, S.; Strekowski, R.; Barbati, S.; Vione, D. Environmental Implications of Hydroxyl Radicals ($\cdot\text{OH}$). *Chem. Rev.* **2015**, *115* (24), 13051–13092.
- (8) Vejerano, E. P.; Rao, G.; Khachatryan, L.; Cormier, S. A.; Lomnicki, S. Environmentally Persistent Free Radicals: Insights on a New Class of Pollutants. *Environ. Sci. Technol.* **2018**, *52* (5), 2468–2481.
- (9) Linn, S. DNA Damage by Iron and Hydrogen Peroxide. In *Advances in DNA Damage and Repair*; Springer US: Boston, MA, 1999; pp 259–266.
- (10) Davies, K. J. A.; Pryor, W. A. The Evolution of Free Radical Biology & Medicine: A 20-Year History. *Free Radic. Biol. Med.* **2005**, *39* (10), 1263–1264.
- (11) Crossley, S. W. M.; Obradors, C.; Martinez, R. M.; Shenvi, R. A. Mn-, Fe-, and Co-Catalyzed Radical Hydrofunctionalizations of Olefins. *Chem. Rev.* **2016**, *116* (15), 8912–9000.
- (12) Yan, M.; Lo, J. C.; Edwards, J. T.; Baran, P. S. Radicals: Reactive Intermediates with Translational Potential. *J. Am. Chem. Soc.* **2016**, *138* (39), 12692–12714.
- (13) *Conjugated Carbon Centered Radicals, High-Spin System and Carbenes*; Fischer, H., Ed.; Landolt-Börnstein - Group II Molecules and Radicals; Springer-Verlag: Berlin/Heidelberg, 2002; Vol. 26B.
- (14) Trinquier, G.; Malrieu, J.-P. Spreading out Spin Density in Polyphenalenyl Radicals. *Phys. Chem. Chem. Phys.* **2017**, *19* (40), 27623–27642.
- (15) Dougherty, D. A. Spin Control in Organic Molecules. *Acc. Chem. Res.* **1991**, *24* (3), 88–94.

- (16) Rajca, A. Organic Diradicals and Polyradicals: From Spin Coupling to Magnetism? *Chem. Rev.* **1994**, *94* (4), 871–893..
- (17) Iwamura, H.; Koga, N. Studies of Organic Di-, Oligo-, and Polyradicals by Means of Their Bulk Magnetic Properties. *Acc. Chem. Res.* **1993**, *26* (6), 346–351.
- (18) Hoffmann, R. Interaction of Orbitals through Space and through Bonds. *Acc. Chem. Res.* **1971**, *4* (1), 1–9.
- (19) Sah, C.; Jacob, L.; Saraswat, M.; Venkataramani, S. Does a Nitrogen Lone Pair Lead to Two Centered–Three Electron (2c–3e) Interactions in Pyridyl Radical Isomers? *J. Phys. Chem. A* **2017**, *121* (19), 3781–3791.
- (20) Lu, D.; Wu, C.; Li, P. 3-Center-5-Electron Boryl Radicals with $\sigma^0 \pi^1$ Ground State Electronic Structure. *Org. Lett.* **2014**, *16* (5), 1486–1489.
- (21) Mukhopadhyay, A.; Jacob, L.; Venkataramani, S. Dehydro-Oxazole, Thiazole and Imidazole Radicals: Insights into the Electronic Structure, Stability and Reactivity Aspects. *Phys. Chem. Chem. Phys.* **2017**, *19* (1), 394–407.
- (22) McFadden, B. D.; Arce, M. M.; Carnicom, E. M.; Herman, J.; Abrusezze, J.; Tillman, E. S. Radical Trap-Assisted Atom Transfer Radical Coupling of Diblock Copolymers as a Method of Forming Triblock Copolymers. *Macromol. Chem. Phys.* **2016**, *217* (22), 2473–2482.
- (23) Mackie, I. D.; DiLabio, G. A. Ring-Opening Radical Clock Reactions: Many Density Functionals Have Difficulty Keeping Time. *Org. Biomol. Chem.* **2011**, *9* (9), 3158.
- (24) Buettner, G. R. The Spin Trapping of Superoxide and Hydroxyl Free Radicals with DMPO (5,5-Dimethylpyrroline-N-Oxide): More about Iron. *Free Radic. Res. Commun.* **1993**, *19 Suppl 1*, S79-87.
- (25) Cristian, A.-M. C.; Shao, Y.; Krylov, A. I. Bonding Patterns in Benzene Triradicals from Structural, Spectroscopic, and Thermochemical Perspectives. *J. Phys. Chem. A* **2004**, *108* (31), 6581–6588.
- (26) Ma, H.; Liu, C.; Zhang, C.; Jiang, Y. Theoretical Study of Very High Spin Organic π -Conjugated Polyradicals \uparrow . *J. Phys. Chem. A* **2007**, *111* (38), 9471–9478.
- (27) Slipchenko, L. V.; Munsch, T. E.; Wenthold, P. G.; Krylov, A. I. 5-Dehydro-1,3-Quinodimethane: A Hydrocarbon with an Open-Shell Doublet Ground State. *Angew. Chemie Int. Ed.* **2004**, *43* (6), 742–745.
- (28) Shimazaki, Y.; Huth, S.; Odani, A.; Yamauchi, O. A Structural Model for the Galactose Oxidase Active Site Which Shows Counteranion-Dependent Phenoxyl Radical Formation by Disproportionation. *Angew. Chemie Int. Ed.* **2000**, *39* (9), 1666–1669.
- (29) Spanget-Larsen, J.; Gil, M.; Gorski, A.; Blake, D. M.; Waluk, J.; Radziszewski, J. G. Vibrations of the Phenoxyl Radical. *J. Am. Chem. Soc.* **2001**, *123* (45), 11253–11261.
- (30) Altwicker, E. R. The Chemistry of Stable Phenoxyl Radicals. *Chem. Rev.* **1967**, *67* (5), 475–531.

- (31) Kreilick, R. W. Nuclear Magnetic Resonance Studies of Phenoxy Radicals. Spin Delocalization in Cyclic Aliphatic Substituents. *J. Am. Chem. Soc.* **1968**, *90* (22), 5991–5996.
- (32) Mahoney, L. R.; DaRooge, M. A. Kinetic Behavior and Thermochemical Properties of Phenoxy Radicals. *J. Am. Chem. Soc.* **1975**, *97* (16), 4722–4731.
- (33) Liu, R.; Morokuma, K.; Mebel, A. M.; Lin, M. C. *Ab Initio* Study of the Mechanism for the Thermal Decomposition of the Phenoxy Radical. *J. Phys. Chem.* **1996**, *100* (22), 9314–9322..
- (34) Schmoltner, A. M.; Anex, D. S.; Lee, Y. T. Infrared Multiphoton Dissociation of Anisole: Production and Dissociation of Phenoxy Radical. *J. Phys. Chem.* **1992**, *96* (3),
- (35) Kröger-Ohlsen, M. V.; Carlsen, C. U.; Andersen, M. L.; Skibsted, L. H. Pseudoperoxidase Activity of Myoglobin: Pigment Catalyzed Formation of Radicals in Meat Systems; 2002; pp 138–150.
- (36) Herrmann, W. A. N-Heterocyclic Carbenes: A New Concept in Organometallic Catalysis. *Angew. Chemie Int. Ed.* **2002**, *41* (8), 1290–1309.
- (37) Hahn, F. E.; Jahnke, M. C. Heterocyclic Carbenes: Synthesis and Coordination Chemistry. *Angew. Chemie Int. Ed.* **2008**, *47* (17), 3122–3172.
- (38) De Sarkar, S.; Grimme, S.; Studer, A. NHC Catalyzed Oxidations of Aldehydes to Esters: Chemoselective Acylation of Alcohols in Presence of Amines. *J. Am. Chem. Soc.* **2010**, *132* (4), 1190–1191.
- (39) Watanabe, T.; Hirose, D.; Curran, D. P.; Taniguchi, T. Borylative Radical Cyclizations of Benzo[3,4]Cyclodec-3-Ene-1,5-Diynes and N-Heterocyclic Carbene-Boranes. *Chem. - A Eur. J.* **2017**, *23* (23), 5404–5409..
- (40) Frisch, M. J.; Trucks, G. W.; Schlegel, H. B.; Scuseria, G. E.; Robb, M. A.; Cheeseman, J. R.; Scalmani, G.; Barone, V.; Petersson, G. A.; Nakatsuji, H.; et al. Gaussian 09, revision C. 01; Gaussian, Inc.: Wallingford, CT, 2009.
- (41) Hohenberg, P.; Kohn, W. Inhomogeneous Electron Gas. *Phys. Rev.* **1964**, *136* (3B), B864–B871.
- (42) West, D.; Sun, Y. Y.; Zhang, S. B. Importance of the Correct Fermi Energy on the Calculation of Defect Formation Energies in Semiconductors. *Appl. Phys. Lett.* **2012**, *101* (8), 082105..
- (43) W. Kohn, *; A. D. Becke, † and; Parr‡, R. G. Density Functional Theory of Electronic Structure. **1996**.
- (44) Becke, A. D. Density-functional Thermochemistry. III. The Role of Exact Exchange. *J. Chem. Phys.* **1993**, *98* (7), 5648–5652..
- (45) Wallace, A. J.; Crittenden, D. L. Optimal Composition of Atomic Orbital Basis Sets for Recovering Static Correlation Energies. *J. Phys. Chem. A* **2014**, *118* (11), 2138–2148.

- (46) Varandas, A. J. C.; Pansini, F. N. N. Optimal Basis Sets for CBS Extrapolation of the Correlation Energy: $OV_x Z$ and $OV(x+d)Z$. *J. Chem. Phys.* **2019**, *150* (15), 154106.
- (47) Matthews, D. A.; Stanton, J. F. A New Approach to Approximate Equation-of-Motion Coupled Cluster with Triple Excitations. *J. Chem. Phys.* **2016**, *145* (12), 124102.
- (48) Zhao, Y.; Truhlar, D. G. The M06 Suite of Density Functionals for Main Group Thermochemistry, Thermochemical Kinetics, Noncovalent Interactions, Excited States, and Transition Elements: Two New Functionals and Systematic Testing of Four M06-Class Functionals and 12 Other Functionals. *Theor. Chem. Acc.* **2008**, *120* (1–3), 215–241.
- (49) Carpenter, J. E.; Weinhold, F. Analysis of the Geometry of the Hydroxymethyl Radical by the Different Hybrids for Different Spins Natural Bond Orbital Procedure. *J. Mol. Struct.: THEOCHEM* **1988**, *169*, 41–62.
- (50) Foster, J. P.; Weinhold, F. Natural Hybrid Orbitals. *J. Am. Chem. Soc.* **1980**, *102*, 7211–7218

Appendix

Table A1: Electronic and thermodynamic parameters of all the radical isomers and their respective parents at both (U)B3LYP/cc-pVTZ and (U)M06-2X/cc-pVTZ levels of theory. Bold font indicates (U)B3LYP and italics represent (U)M06-2X.

Species	Absolute energy (Hartrees)	ZPVE (Hartrees)	Lowest frequency	Spin Contamination		Point group	Electronic state	Absolute free energy (G) (Hartrees)	Absolute Enthalpy (H) (Hartrees)
				Before annihilation	After annihilation				
1	-323.547043	0.093351	216.50	0.0000	0.0000	C _s	¹ A'	-323.575824	-323.540902
	<i>-323.414239</i>	<i>0.094426</i>	<i>220.28</i>	<i>0.0000</i>	<i>0.0000</i>		¹ A'	<i>-323.442999</i>	<i>-323.408126</i>
1O	-322.898140	0.079363	154.36	0.7859	0.7509	C _s	² A''	-322.927705	-322.892014
	<i>-322.760125</i>	<i>0.080199</i>	<i>154.62</i>	<i>0.7923</i>	<i>0.7511</i>		² A''	<i>-322.789674</i>	<i>-322.754024</i>
1α'	-322.878358	0.080438	215.57	0.7556	0.7500	C _s	² A'	-322.907728	-322.872229
	<i>-322.747803</i>	<i>0.081456</i>	<i>218.92</i>	<i>0.7597</i>	<i>0.7500</i>		² A'	<i>-322.777142</i>	<i>-322.741719</i>
1β	-322.867802	0.080475	218.19	0.7577	0.7500	C _s	² A'	-322.897182	-322.861691
	<i>-322.736654</i>	<i>0.081602</i>	<i>222.39</i>	<i>0.7631</i>	<i>0.7501</i>		² A'	<i>-322.766006</i>	<i>-322.730582</i>
1β'	-322.867403	0.080336	231.56	0.7570	0.7500	C _s	² A'	-322.896778	-322.861267
	<i>-322.737254</i>	<i>0.081428</i>	<i>235.17</i>	<i>0.7619</i>	<i>0.7501</i>		² A'	<i>-322.766599</i>	<i>-322.731163</i>
1γ	-322.871391	0.080087	212.99	0.7562	0.7500	C _s	² A'	-322.900762	-322.865263
	<i>-322.741813</i>	<i>0.081262</i>	<i>216.24</i>	<i>0.7612</i>	<i>0.7501</i>		² A'	<i>-322.771153</i>	<i>-322.735733</i>
2	-323.532078	0.092750	229.59	0.0000	0.0000	C _s	¹ A'	-323.560981	-323.525770
	<i>-323.398804</i>	<i>0.093791</i>	<i>233.88</i>	<i>0.0000</i>	<i>0.0000</i>		¹ A'	<i>-323.427700</i>	<i>-323.392510</i>
2O	-322.897173	0.079273	184.36	0.7854	0.7508	C _s	² A''	-322.926686	-322.891031
	<i>-322.759686</i>	<i>0.080138</i>	<i>185.93</i>	<i>0.7902</i>	<i>0.7510</i>		² A''	<i>-322.789173</i>	<i>-322.753579</i>
2α	-322.867590	0.080266	226.92	0.7555	0.7500	C _s	² A'	-322.897044	-322.861353
	<i>-322.735091</i>	<i>0.081200</i>	<i>232.62</i>	<i>0.7582</i>	<i>0.7500</i>		² A'	<i>-322.764533</i>	<i>-322.728873</i>
2α'	-322.862948	0.079908	246.14	0.7555	0.7500	C _s	² A'	-322.892456	-322.856627
	<i>-322.731660</i>	<i>0.080864</i>	<i>250.80</i>	<i>0.7593</i>	<i>0.7500</i>		² A'	<i>-322.761144</i>	<i>-322.725377</i>
2β'	-322.855729	0.079703	223.41	0.7570	0.7500	C _s	² A'	-322.885236	-322.849431
	<i>-322.724373</i>	<i>0.080815</i>	<i>229.21</i>	<i>0.7623</i>	<i>0.7501</i>		² A'	<i>-322.753855</i>	<i>-322.718116</i>
2γ	-322.853636	0.079655	226.16	0.7569	0.7500	C _s	² A'	-322.883153	-322.847341
	<i>-322.722858</i>	<i>0.080849</i>	<i>231.33</i>	<i>0.7622</i>	<i>0.7501</i>		² A'	<i>-322.752364</i>	<i>-322.716592</i>
3	-323.535603	0.092995	228.69	0.0000	0.0000	C _s	¹ A'	-323.564474	-323.529345
	<i>-323.402646</i>	<i>0.094059</i>	<i>230.67</i>	<i>0.0000</i>	<i>0.0000</i>		¹ A'	<i>-323.431499</i>	<i>-323.396413</i>
3O	-322.891855	0.079137	191.63	0.7920	0.7512	C _{2v}	² B ₁	-322.920687	-322.885742
	<i>-322.752984</i>	<i>0.079751</i>	<i>192.78</i>	<i>0.7969</i>	<i>0.7515</i>		² B ₁	<i>-322.781794</i>	<i>-322.746898</i>
3α	-322.868740	0.080207	224.84	0.7552	0.7500	C _s	² A'	-322.898198	-322.862496
	<i>-322.737667</i>	<i>0.081212</i>	<i>226.84</i>	<i>0.7586</i>	<i>0.7500</i>		² A'	<i>-322.767095</i>	<i>-322.731469</i>
3β	-322.858054	0.080261	225.39	0.7568	0.7500	C _s	² A'	-322.887526	-322.851833
	<i>-322.726437</i>	<i>0.081378</i>	<i>228.84</i>	<i>0.7612</i>	<i>0.7501</i>		² A'	<i>-322.755880</i>	<i>-322.720260</i>

Table A2: Electronic and thermodynamic parameters of all the singlet and triplet biradical isomers and their respective parents at (U)B3LYP/cc-pVTZ level of theory. Bold font indicates singlet state and italics represent triplet state.

Species	Absolute energy (Hartrees)	ZPVE (Hartrees)	Lowest frequency	Spin Contamination		Point group	Electronic state	Absolute free energy (G) (Hartrees)	Absolute Enthalpy (H) (Hartrees)
				Before annihilation	After annihilation				
1O β	-322.222904	0.066464	153.22	0.0000	0.0000	C _s	³A''	-322.252793	-322.216819
	<i>-322.222904</i>	<i>0.066464</i>	<i>153.22</i>	<i>2.0463</i>	<i>2.0010</i>	C _s	<i>³A''</i>	<i>-322.252793</i>	<i>-322.216819</i>
1O γ	-322.280582	0.065499	78.82	0.0000	0.0000	C ₁	¹A	-322.311939	-322.272860
	<i>-322.224009</i>	<i>0.066138</i>	<i>146.29</i>	<i>2.0240</i>	<i>2.0003</i>	C _s	<i>³A''</i>	<i>-322.253915</i>	<i>-322.217896</i>
1O β'	-322.198849	0.064607	128.16	0.0000	0.0000	C ₁	¹A	-322.227658	-322.192779
	<i>-322.223096</i>	<i>0.066626</i>	<i>162.82</i>	<i>2.0457</i>	<i>2.0010</i>	C _s	<i>³A''</i>	<i>-322.252959</i>	<i>-322.217021</i>
1O α'	-322.300876	0.065735	69.44	0.0000	0.0000	C _s	¹A'	-322.332190	-322.293260
	<i>-322.237495</i>	<i>0.066483</i>	<i>152.09</i>	<i>2.0303</i>	<i>2.0004</i>	C _s	<i>³A''</i>	<i>-322.267408</i>	<i>-322.231337</i>
1 $\beta\gamma$	-322.234599	0.068407	218.97	0.0000	0.0000	C _s	¹A'	-322.263220	-322.228502
	<i>-322.177978</i>	<i>0.067527</i>	<i>203.19</i>	<i>2.0071</i>	<i>2.0000</i>	C _s	<i>³A'</i>	<i>-322.207751</i>	<i>-322.171810</i>
1 $\beta\beta'$	-322.195880	0.066242	207.39	0.0000	0.0000	C _s	¹A'	-322.224954	-322.189246
	<i>-322.187609</i>	<i>0.067612</i>	<i>234.31</i>	<i>2.0202</i>	<i>2.0002</i>	C _s	<i>³A'</i>	<i>-322.217306</i>	<i>-322.181514</i>
1 $\beta\alpha'$	-322.199594	0.066520	227.65	0.0000	0.0000	C _s	¹A'	-322.228248	-322.193389
	<i>-322.193746</i>	<i>0.067720</i>	<i>205.06</i>	<i>2.0071</i>	<i>2.0000</i>	C _s	<i>³A'</i>	<i>-322.223493</i>	<i>-322.187614</i>
1 βO	-322.301264	0.068208	144.27	0.0000	0.0000	C _s	¹A'	-322.330610	-322.294975
	<i>-322.222904</i>	<i>0.066464</i>	<i>153.22</i>	<i>2.0463</i>	<i>2.0010</i>	C _s	<i>³A''</i>	<i>-322.252793</i>	<i>-322.216819</i>
1 $\gamma\beta'$	-322.227880	0.068153	250.24	0.0000	0.0000	C _s	¹A'	-322.256541	-322.221678
	<i>-322.180317</i>	<i>0.067203</i>	<i>215.95</i>	<i>2.0081</i>	<i>2.0000</i>	C _s	<i>³A'</i>	<i>-322.210069</i>	<i>-322.174136</i>
1 $\gamma\alpha'$	-322.221954	0.066736	207.10	0.0000	0.0000	C _s	¹A'	-322.250664	-322.215684
	<i>-322.195550</i>	<i>0.067364</i>	<i>208.14</i>	<i>2.0149</i>	<i>2.0001</i>	C _s	<i>³A'</i>	<i>-322.225271</i>	<i>-322.189398</i>
1 γO	-322.280584	0.065497	79.09	0.0000	0.0000	C ₁	¹A	-322.311930	-322.272866
	<i>-322.224009</i>	<i>0.066138</i>	<i>146.29</i>	<i>2.0240</i>	<i>2.0003</i>	C _s	<i>³A''</i>	<i>-322.253915</i>	<i>-322.217896</i>
1 $\gamma\beta$	-322.234599	0.068407	218.97	0.0000	0.0000	C _s	¹A'	-322.263220	-322.228502
	<i>-322.177978</i>	<i>0.067527</i>	<i>203.19</i>	<i>2.0071</i>	<i>2.0000</i>	C _s	<i>³A'</i>	<i>-322.207751</i>	<i>-322.171810</i>
1 $\beta'\gamma'$	-322.224293	0.068057	245.97	0.0000	0.0000	C _s	¹A'	-322.252951	-322.218105
	<i>-322.195524</i>	<i>0.067820</i>	<i>232.52</i>	<i>2.0091</i>	<i>2.0000</i>	C _s	<i>³A'</i>	<i>-322.225223</i>	<i>-322.189396</i>
1 $\beta'\text{O}$	-322.198849	0.064607	127.92	0.0000	0.0000	C _s	¹A	-322.227658	-322.192779
	<i>-322.223096</i>	<i>0.066626</i>	<i>162.82</i>	<i>2.0457</i>	<i>2.0010</i>	C _s	<i>³A'</i>	<i>-322.252959</i>	<i>-322.217021</i>
1 $\beta'\beta$	-322.195880	0.066242	207.39	0.0000	0.0000	C _s	¹A'	-322.224954	-322.189246
	<i>-322.187609</i>	<i>0.067612</i>	<i>234.31</i>	<i>2.0202</i>	<i>2.0002</i>	C _s	<i>³A'</i>	<i>-322.217306</i>	<i>-322.181514</i>
1 $\beta'\gamma$	-322.227880	0.068153	250.24	0.0000	0.0000	C _s	¹A'	-322.256541	-322.221678
	<i>-322.180317</i>	<i>0.067203</i>	<i>215.95</i>	<i>2.0081</i>	<i>2.0000</i>	C _s	<i>³A'</i>	<i>-322.210069</i>	<i>-322.174136</i>
1 $\alpha'\text{O}$	-322.300876	0.065735	69.43	0.0000	0.0000	C _s	¹A'	-322.332190	-322.293260
	<i>-322.237495</i>	<i>0.066483</i>	<i>152.09</i>	<i>2.0303</i>	<i>2.0004</i>	C _s	<i>³A''</i>	<i>-322.267408</i>	<i>-322.231337</i>

Species	Absolute energy (Hartrees)	ZPVE (Hartrees)	Lowest frequency	Spin Contamination		Point group	Electronic state	Absolute free energy (G) (Hartrees)	Absolute Enthalpy (H) (Hartrees)
				Before annihilation	After annihilation				
1 α' β	-322.199594	0.066520	227.65	0.0000	0.0000	C _s	¹A'	-322.228248	-322.193389
	-322.193746	0.067720	205.06	2.0071	2.0000	C _s	³ A'	-322.223493	-322.187614
1 α' γ	-322.221954	0.066736	207.10	0.0000	0.0000	C _s	¹A'	-322.250664	-322.215684
	-322.195550	0.067365	208.14	2.0149	2.0001	C _s	³ A'	-322.225271	-322.189398
1 α' β'	-322.224293	0.068057	245.97	0.0000	0.0000	C _s	¹A'	-322.252951	-322.218105
	-322.195524	0.067820	232.52	2.0091	2.0000	C _s	³ A'	-322.225223	-322.189396
2O γ	-322.302301	0.062801	134.39	0.0000	0.0000	C ₁	¹A	-322.331716	-322.295975
	-322.221395	0.066204	174.54	2.0478	2.0011	C _s	³ A''	-322.251244	-322.215299
2O β'	-322.227293	0.065137	173.56	0.0000	0.0000	C _s	¹A'	-322.256184	-322.220893
	-322.223118	0.066110	169.57	2.0250	2.0003	C _s	³ A''	-322.253006	-322.216954
2O α'	-322.220026	0.065443	576.19(img)	0.0000	0.0000	C _s	¹A'	-322.248699	-322.214022
	-322.231034	0.066801	201.19	2.0375	2.0007	C _s	³ A''	-322.260804	-322.224980
2O α	-322.247440	0.066542	143.67	0.0000	0.0000	C _s	¹A'	-322.276376	-322.241167
	-322.232398	0.066535	167.46	2.0405	2.0008	C _s	³ A''	-322.262274	-322.226271
2 $\gamma\beta'$	-322.221898	0.067892	222.62	0.0000	0.0000	C _s	¹A'	-322.250643	-322.215650
	-322.162323	0.066931	210.27	2.0076	2.0000	C _s	³ A'	-322.192268	-322.155949
2 $\gamma\alpha'$	-322.199602	0.066424	255.00	0.0000	0.0000	C _s	¹A'	-322.228449	-322.193169
	-322.178319	0.066993	231.38	2.0158	2.0001	C _s	³ A'	-322.208206	-322.171980
2 $\gamma\alpha'$	-322.213303	0.067023	235.26	0.0000	0.0000	C _s	¹A'	-322.242052	-322.207022
	-322.180056	0.067470	203.02	2.0135	2.0001	C _s	³ A'	-322.173761	-322.209938
2 γ O	-322.302294	0.068207	133.83	0.0000	0.0000	C _s	¹A'	-322.331712	-322.295968
	-322.221393	0.066206	174.35	2.0478	2.0011	C _s	³ A''	-322.251244	-322.215296
2 $\beta'\alpha'$	-322.209776	0.067351	276.40	0.0000	0.0000	C _s	¹A'	-322.238575	-322.203408
	-322.185094	0.067376	237.77	2.0101	2.0001	C _s	³ A'	-322.214920	-322.178807
2 $\beta'\alpha$	-322.191854	0.066192	230.58	0.0000	0.0000	C _s	¹A'	-322.220639	-322.185487
	-322.185644	0.067390	214.17	2.0080	2.0000	C _s	³ A'	-322.215455	-322.179404
2 β' O	-322.227293	0.065137	173.57	0.0000	0.0000	C _s	¹A'	-322.256183	-322.220893
	-322.223118	0.066111	169.50	2.0250	2.0003	C _s	³ A''	-322.253006	-322.216954
2 $\beta'\gamma$	-322.221898	0.067892	222.61	0.0000	0.0000	C _s	¹A'	-322.250642	-322.215649
	-322.162322	0.066931	210.23	2.0076	2.0000	C _s	³ A'	-322.192267	-322.155948
2 $\alpha'\alpha$	-322.176302	0.064849	236.92	0.0000	0.0000	C _s	¹A'	-322.205435	-322.169538
	-322.194870	0.067707	248.39	2.0146	2.0001	C _s	³ A'	-322.224643	-322.188684
2 α' O	-322.220025	0.065444	576.28(img)	0.0000	0.0000	C _s	¹A'	-322.248699	-322.214022
	-322.231034	0.066801	201.19	2.0375	2.0007	C _s	³ A''	-322.260804	-322.224980
2 $\alpha'\gamma$	-322.199602	0.066424	254.99	0.0000	0.0000	C _s	¹A'	-322.228449	-322.193169
	-322.178319	0.066993	231.38	2.0158	2.0001	C _s	³ A'	-322.208205	-322.171980
2 $\alpha'\beta'$	-322.209776	0.67351	276.40	0.0000	0.0000	C _s	¹A'	-322.238575	-322.203408
	-322.185094	0.067377	237.77	2.0101	2.0001	C _s	³ A'	-322.214919	-322.178807

Species	Absolute energy (Hartrees)	ZPVE (Hartrees)	Lowest frequency	Spin Contamination		Point group	Electronic state	Absolute free energy (G) (Hartrees)	Absolute Enthalpy (H) (Hartrees)
				Before annihilation	After annihilation				
2 α O	-322.247442	0.065542	143.60	0.0000	0.0000	C _s	¹ A'	-322.276376	-322.241167
	-322.232398	0.066535	167.46	2.0405	2.0008	C _s	³ A''	-322.262274	-322.226271
2 α γ	-322.213303	0.067022	235.32	0.0000	0.0000	C _s	¹ A'	-322.242053	-322.207023
	-322.180056	0.067470	203.01	2.0135	2.0001	C _s	³ A'	-322.209938	-322.173761
2 α β '	-322.191854	0.066191	230.64	0.0000	0.0000	C _s	¹ A'	-322.220639	-322.185488
	-322.185644	0.067390	214.17	2.0089	2.0000	C _s	³ A'	-322.215455	-322.179404
2 α α '	-322.176302	0.064849	236.94	0.0000	0.0000	C _s	¹ A'	-322.205434	-322.169538
	-322.194870	0.067707	248.39	2.0146	2.0001	C _s	³ A'	-322.224623	-322.188684
3O β	-322.302295	0.068207	134.06	0.0000	0.0000	C _s	¹ A'	-322.331711	-322.295969
	-322.214279	0.066274	181.29	2.0579	2.0016	C _s	³ A''	-322.244122	-322.208193
3O α	-322.251151	0.066334	160.37	0.0000	0.0000	C _s	¹ A'	-322.280147	-322.244741
	-322.224155	0.066224	188.37	2.0318	2.0005	C _s	³ A''	-322.253956	-322.218062
3 β O	-322.302294	0.068207	133.51	0.0000	0.0000	C _s	¹ A'	-322.331751	-322.295966
	-322.214279	0.066274	181.30	2.0579	2.0016	C _s	³ A''	-322.244123	-322.208193
3 β β '	-322.204849	0.067310	159.22	0.0000	0.0000	C _s	¹ A'	-322.233831	-322.198453
	-322.177035	0.067685	214.00	2.0183	2.0002	C _s	³ A'	-322.206844	-322.170856
3 β α '	-322.194052	0.066306	238.13	0.0000	0.0000	C _s	¹ A'	-322.222847	-322.187653
	-322.186283	0.067558	214.13	2.0072	2.0000	C _s	³ A'	-322.216108	-322.180055
3 β α	-322.230083	0.068456	216.32	0.0000	0.0000	C _s	¹ A'	-322.258710	-322.224017
	-322.189426	0.068033	226.44	2.0093	2.0000	C _s	³ A'	-322.219186	-322.183254
3 α O	-322.251151	0.066334	160.39	0.0000	0.0000	C _s	¹ A'	-322.280146	-322.244741
	-322.224155	0.066224	188.38	2.0318	2.0005	C _s	³ A''	-322.218062	-322.253956
3 α β '	-322.188038	0.066000	233.55	0.0000	0.0000	C _s	¹ A'	-322.216888	-322.181565
	-322.184122	0.067502	209.90	2.0073	2.0000	C _s	³ A'	-322.213969	-322.177869
3 α α '	-322.192976	0.066266	183.81	0.0000	0.0000	C _s	¹ A'	-322.221761	-322.186638
	-322.199141	0.067734	224.42	2.0138	2.0001	C _s	³ A'	-322.228883	-322.192969
3 α β	-322.230083	0.068456	216.32	0.0000	0.0000	C _s	¹ A'	-322.258710	-322.224017
	-322.189426	0.068033	226.44	2.0093	2.0000	C _s	³ A'	-322.219186	-322.183254

Table A3: Cartesian coordinates of the optimized structures at different levels of theory.

(U)B3LYP/cc-pVTZ				(U)M06-2X/cc-pVTZ			
1				1			
C	0.000000	0.901655	0.000000	C	0.000000	0.898809	0.000000
C	-1.224089	0.226840	0.000000	C	-1.222063	0.223956	0.000000
C	-1.190411	-1.154154	0.000000	C	-1.185977	-1.153095	0.000000
C	0.038515	-1.813353	0.000000	C	0.042468	-1.809416	0.000000
C	1.188133	-1.042306	0.000000	C	1.187296	-1.037040	0.000000
N	1.176435	0.294831	0.000000	N	1.174585	0.297965	0.000000
H	-2.114715	-1.716600	0.000000	H	-2.109048	-1.717174	0.000000
H	0.100480	-2.891709	0.000000	H	0.107735	-2.886881	0.000000
H	2.167247	-1.507019	0.000000	H	2.167067	-1.499355	0.000000
O	-0.004333	2.253387	0.000000	H	-0.010718	2.245644	0.000000
H	-2.149055	0.783939	0.000000	H	-2.144381	0.784662	0.000000
H	0.922779	2.528380	0.000000	H	0.911934	2.528558	0.000000
1O				1O			
C	0.000000	1.015051	0.000000	C	0.000000	1.015213	0.000000
C	-1.224263	0.236253	0.000000	C	-1.223114	0.232874	0.000000
C	-1.172159	-1.137999	0.000000	C	-1.171030	-1.138609	0.000000
C	0.078860	-1.748949	0.000000	C	0.078821	-1.743947	0.000000
C	1.241656	-0.935324	0.000000	C	1.243096	-0.926778	0.000000
N	1.234957	0.368693	0.000000	N	1.236713	0.370181	0.000000
H	-2.077060	-1.730948	0.000000	H	-2.074566	-1.732563	0.000000
H	0.179144	-2.825354	0.000000	H	0.183976	-2.819206	0.000000
H	2.215536	-1.417034	0.000000	H	2.215631	-1.410103	0.000000
O	-0.043824	2.254418	0.000000	H	-0.049502	2.244330	0.000000
H	-2.156297	0.782951	0.000000	H	-2.152647	0.783446	0.000000
1α'				1α'			
C	0.000000	0.887522	0.000000	C	0.000000	0.881898	0.000000
C	-1.178852	0.143286	0.000000	C	-1.177378	0.139060	0.000000
C	-1.077299	-1.240149	0.000000	C	-1.072950	-1.240469	0.000000
C	0.175007	-1.860953	0.000000	C	0.178802	-1.855487	0.000000
C	1.245369	-0.990664	0.000000	C	1.243341	-0.983691	0.000000
N	1.198713	0.296409	0.000000	N	1.200654	0.306296	0.000000
O	-0.051844	2.232747	0.000000	O	-0.060239	2.222555	0.000000
H	0.859218	2.555577	0.000000	H	0.847000	2.551136	0.000000
H	-2.132564	0.648959	0.000000	H	-2.128857	0.647993	0.000000
H	-1.977665	-1.842165	0.000000	H	-1.971297	-1.844654	0.000000
H	0.289423	-2.933456	0.000000	H	0.299599	-2.926852	0.000000

(U)B3LYP/cc-pVTZ				(U)M06-2X/cc-pVTZ			
1β				1β			
C	0.000000	0.943636	0.000000	C	0.000000	0.936747	0.000000
C	1.210493	0.274953	0.000000	C	1.212946	0.271279	0.000000
C	1.301225	-1.083166	0.000000	C	1.295929	-1.085629	0.000000
C	0.096928	-1.805682	0.000000	C	0.090699	-1.798646	0.000000
C	-1.083589	-1.083564	0.000000	C	-1.085498	-1.074538	0.000000
N	-1.133739	0.252497	0.000000	N	-1.135686	0.260031	0.000000
H	2.257118	-1.591941	0.000000	H	2.250338	-1.596426	0.000000
H	0.088203	-2.886622	0.000000	H	0.075109	-2.878583	0.000000
H	-2.041255	-1.590247	0.000000	H	-2.043255	-1.580170	0.000000
O	-0.064320	2.288090	0.000000	O	-0.053503	2.277745	0.000000
H	-1.003675	2.519556	0.000000	H	-0.988813	2.517725	0.000000
1β'				1β'			
C	0.000000	0.834756	0.000000	C	0.000000	0.832344	0.000000
C	-1.228489	0.162609	0.000000	C	-1.224387	0.156190	0.000000
C	-1.198276	-1.225332	0.000000	C	-1.191738	-1.226436	0.000000
C	0.043117	-1.818369	0.000000	C	0.050084	-1.818792	0.000000
C	1.214303	-1.112560	0.000000	C	1.212309	-1.101559	0.000000
N	1.179260	0.233524	0.000000	N	1.178934	0.240544	0.000000
H	2.191628	-1.576737	0.000000	H	2.190461	-1.564265	0.000000
O	-0.009469	2.187914	0.000000	O	-0.020648	2.180441	0.000000
H	0.914784	2.471095	0.000000	H	0.898675	2.473165	0.000000
H	-2.153819	0.720492	0.000000	H	-2.147288	0.716986	0.000000
H	-2.115586	-1.799464	0.000000	H	-2.106814	-1.803712	0.000000
1γ				1γ			
C	0.000000	0.870837	0.000000	C	0.000000	0.867641	0.000000
C	-1.271532	0.267777	0.000000	C	-1.268438	0.268171	0.000000
C	-1.246382	-1.093020	0.000000	C	-1.246278	-1.091356	0.000000
C	-0.111370	-1.867454	0.000000	C	-0.108493	-1.862070	0.000000
C	1.079619	-1.142475	0.000000	C	1.077539	-1.139661	0.000000
N	1.136168	0.190747	0.000000	N	1.134624	0.192284	0.000000
H	-0.112542	-2.947365	0.000000	H	-0.111883	-2.941461	0.000000
H	2.031858	-1.661707	0.000000	H	2.030693	-1.655785	0.000000
O	0.072640	2.218450	0.000000	O	0.070992	2.210540	0.000000
H	1.013448	2.442959	0.000000	H	1.008961	2.438813	0.000000
H	-2.169067	0.869289	0.000000	H	2.164055	0.871777	0.000000

(U)B3LYP/cc-pVTZ				(U)M06-2X/cc-pVTZ			
2				2			
C	1.178014	0.172525	0.000000	C	0.174729	0.171290	0.000000
C	0.000000	0.919340	0.000000	C	0.000000	0.916842	0.000000
C	-1.214204	0.242424	0.000000	C	-1.212184	0.243765	0.000000
C	-1.190733	-1.142979	0.000000	C	-1.190226	-1.138814	0.000000
C	0.034361	-1.801844	0.000000	C	0.032881	-1.796898	0.000000
H	2.140646	0.678950	0.000000	H	2.136258	0.678880	0.000000
H	-2.112863	-1.708015	0.000000	H	-2.111587	-1.703913	0.000000
H	0.080984	-2.884101	0.000000	H	0.078884	-2.878606	0.000000
N	1.200076	-1.156725	0.000000	N	1.196417	-1.154746	0.000000
H	-2.139941	0.800940	0.000000	H	-2.134954	0.807089	0.000000
O	-0.013101	2.282228	0.000000	O	-0.008622	2.274678	0.000000
H	0.890823	2.614676	0.000000	H	0.894264	2.605242	0.000000
2O				2O			
C	1.213148	0.223609	0.000000	C	1.211874	0.221637	0.000000
C	0.000000	1.025136	0.000000	C	0.000000	1.023652	0.000000
C	-1.238687	0.286614	0.000000	C	-1.239212	0.287198	0.000000
C	-1.196197	-1.081996	0.000000	C	-1.197091	-1.076834	0.000000
C	0.050865	-1.731054	0.000000	C	0.050340	-1.724841	0.000000
H	2.159669	0.753897	0.000000	H	2.156582	0.754565	0.000000
H	-2.101808	-1.674054	0.000000	H	-2.100803	-1.670402	0.000000
H	0.098480	-2.813447	0.000000	H	0.097092	-2.806562	0.000000
N	1.233478	-1.090873	0.000000	N	1.232023	-1.088703	0.000000
H	-2.165315	0.844315	0.000000	H	-2.163473	0.848673	0.000000
O	0.049983	2.273944	0.000000	O	0.053872	2.263722	0.000000
2α				2α			
C	1.187388	0.221537	0.000000	C	1.180030	0.213804	0.000000
C	0.000000	0.951320	0.000000	C	0.000000	0.949651	0.000000
C	-1.167747	0.196737	0.000000	C	-1.166577	0.203036	0.000000
C	-1.082604	-1.195252	0.000000	C	-1.085189	-1.187125	0.000000
C	0.158934	-1.808264	0.000000	C	0.152988	-1.800021	0.000000
N	1.268218	-1.045330	0.000000	N	1.270434	-1.053690	0.000000
O	-0.058837	2.305830	0.000000	O	-0.049452	2.300335	0.000000
H	0.842022	2.649756	0.000000	H	0.850609	2.641607	0.000000
H	-2.125195	0.701699	0.000000	H	-2.119865	0.715283	0.000000
H	-1.981806	-1.795415	0.000000	H	-1.984852	-1.785494	0.000000
H	0.282328	-2.881838	0.000000	H	0.269174	-2.874311	0.000000

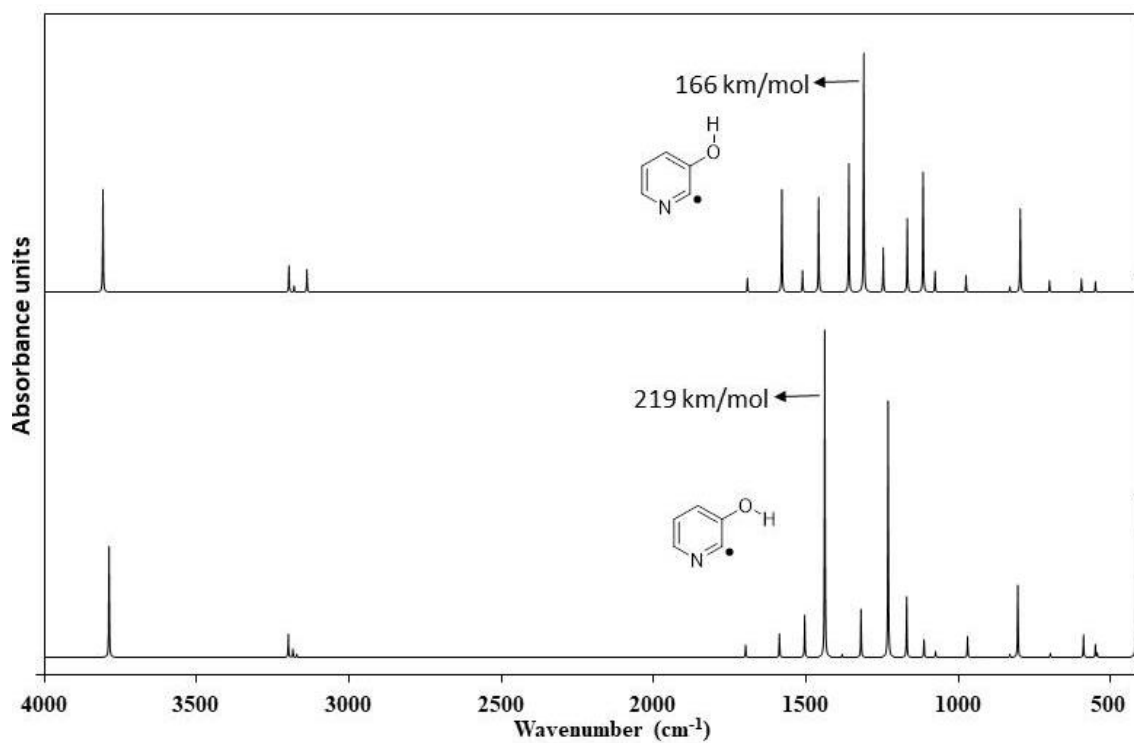
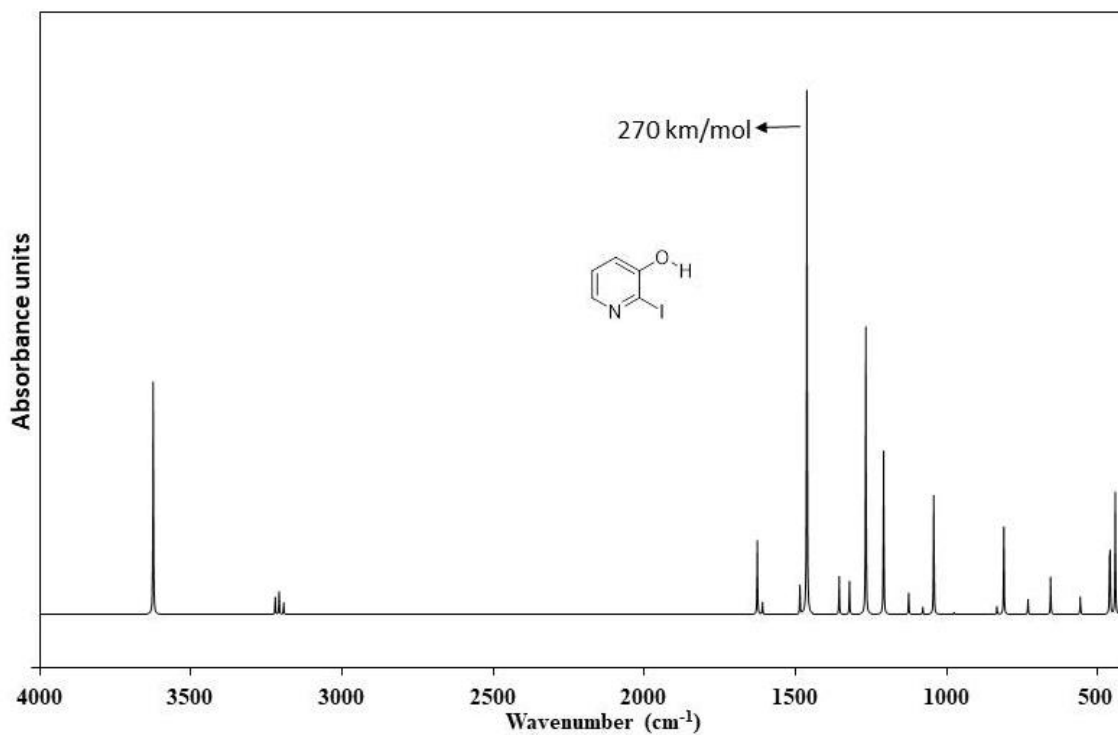
(U)B3LYP/cc-pVTZ				(U)M06-2X/cc-pVTZ			
2α'				2α'			
C	1.196875	0.148682	0.000000	C	1.190521	0.143840	0.000000
C	0.000000	0.855278	0.000000	C	0.000000	0.852005	0.000000
C	-1.205556	0.145504	0.000000	C	-1.205737	0.149210	0.000000
C	-1.178501	-1.240886	0.000000	C	-1.180843	-1.232692	0.000000
C	0.083069	-1.823605	0.000000	C	0.078153	-1.815555	0.000000
H	2.155813	0.656308	0.000000	H	2.147954	0.654417	0.000000
N	1.195418	-1.194732	0.000000	N	1.198706	-1.196495	0.000000
O	-0.062498	2.217567	0.000000	O	-0.055368	2.209948	0.000000
H	0.827047	2.586100	0.000000	H	0.834623	2.573253	0.000000
H	-2.138546	0.693717	0.000000	H	-2.134584	0.704049	0.000000
H	-2.087580	-1.823374	0.000000	H	-2.088558	-1.816697	0.000000
2β'				2β'			
C	1.132426	0.074548	0.000000	C	1.129556	0.070704	0.000000
C	0.000000	0.893444	0.000000	C	0.000000	0.888023	0.000000
C	-1.256067	0.278443	0.000000	C	-1.255747	0.284629	0.000000
C	-1.246203	-1.087612	0.000000	C	-1.250454	-1.080679	0.000000
C	-0.111821	-1.864847	0.000000	C	-0.114098	-1.853239	0.000000
H	2.123118	0.521349	0.000000	H	2.118371	0.521024	0.000000
H	-0.120102	-2.945655	0.000000	H	-0.130743	-2.934225	0.000000
N	1.080717	-1.252407	0.000000	N	1.079621	-1.254149	0.000000
O	0.062280	2.251895	0.000000	O	0.070368	2.241110	0.000000
H	0.982513	2.537146	0.000000	H	0.990846	2.519865	0.000000
H	-2.158803	0.874993	0.000000	H	-2.154316	0.886873	0.000000
2γ				2γ			
C	-1.136452	0.133480	0.000000	C	-1.133413	0.136993	0.000000
C	0.000000	0.958075	0.000000	C	0.000000	0.954287	0.000000
C	1.199456	0.285812	0.000000	C	1.199851	0.285479	0.000000
C	1.305587	-1.072825	0.000000	C	1.300431	-1.073656	0.000000
C	0.098252	-1.788391	0.000000	C	0.095990	-1.783202	0.000000
H	-2.123828	0.592266	0.000000	H	-2.119349	0.597311	0.000000
H	2.255566	-1.590627	0.000000	H	2.250830	-1.589510	0.000000
H	0.107828	-2.872093	0.000000	H	0.099845	-2.866276	0.000000
N	-1.088696	-1.193185	0.000000	N	-1.089065	-1.188249	0.000000
O	-0.055425	2.315849	0.000000	O	-0.051856	2.307877	0.000000
H	-0.976351	2.599044	0.000000	H	-0.970170	2.593791	0.000000

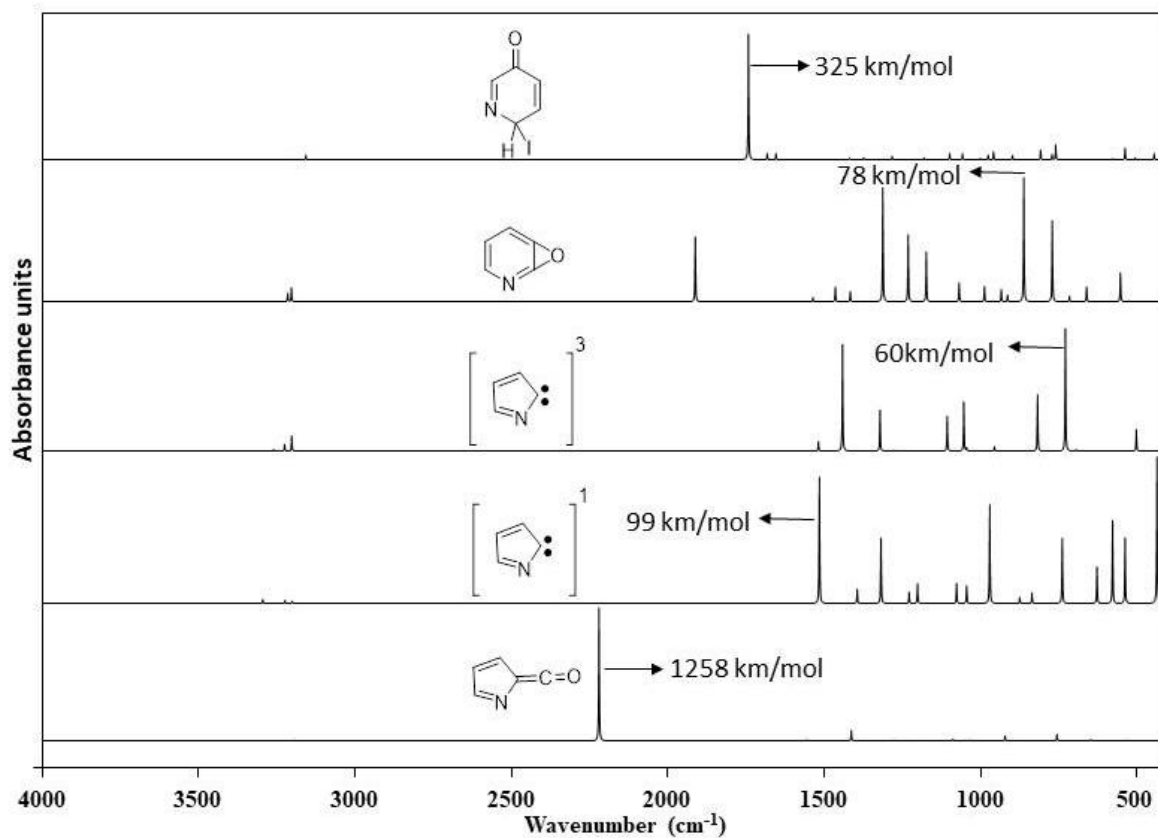
(U)B3LYP/cc-pVTZ				(U)M06-2X/cc-pVTZ			
3				3			
C	-1.117901	-1.180038	0.000000	C	-1.114312	-1.177346	0.000000
C	-1.190117	0.206383	0.000000	C	-1.187788	0.206761	0.000000
C	0.000000	0.929407	0.000000	C	0.000000	0.926925	0.000000
C	1.202528	0.229448	0.000000	C	1.200626	0.230201	0.000000
C	1.151960	-1.156151	0.000000	C	1.149806	-1.152879	0.000000
H	-2.031518	-1.764474	0.000000	H	-2.027090	-1.762136	0.000000
H	-2.150364	0.707279	0.000000	H	-2.146836	0.708818	0.000000
H	2.142969	0.760977	0.000000	H	2.138857	0.764841	0.000000
H	2.075260	-1.724894	0.000000	H	2.072519	-1.721634	0.000000
N	0.022825	-1.869045	0.000000	N	0.023497	-1.864643	0.000000
O	0.046645	2.285961	0.000000	O	0.044555	2.278237	0.000000
H	-0.848100	2.642438	0.000000	H	-0.848364	2.634730	0.000000
3O				3O			
C	0.000000	1.154372	-1.107220	C	0.000000	1.152780	-1.104389
C	0.000000	1.221847	0.266557	C	0.000000	1.220893	0.266765
C	0.000000	0.000000	1.032920	C	0.000000	0.000000	1.030526
C	0.000000	-1.221847	0.266557	C	0.000000	-1.220893	0.266765
C	0.000000	-1.154372	-1.107220	C	0.000000	-1.152780	-1.104389
H	0.000000	2.058793	-1.704122	H	0.000000	2.055775	-1.702178
H	0.000000	2.163945	0.796533	H	0.000000	2.161177	0.799500
H	0.000000	-2.163945	0.796533	H	0.000000	-2.161177	0.799500
H	0.000000	-2.058793	-1.704122	H	0.000000	-2.055775	-1.702178
N	0.000000	0.000000	-1.798692	N	0.000000	0.000000	-1.792567
O	0.000000	0.000000	2.287057	O	0.000000	0.000000	2.277706
3α				3α			
C	1.054829	-1.263823	0.000000	C	1.048373	-1.259832	0.000000
C	1.168066	0.111238	0.000000	C	1.165390	0.111927	0.000000
C	0.000000	0.885468	0.000000	C	0.000000	0.884839	0.000000
C	-1.241956	0.248103	0.000000	C	-1.237748	0.251483	0.000000
C	-1.192861	-1.133784	0.000000	C	-1.186731	-1.128230	0.000000
H	1.931330	-1.898845	0.000000	H	1.925852	-1.893406	0.000000
H	2.133137	0.596120	0.000000	H	2.128989	0.598950	0.000000
N	-0.148775	-1.872480	0.000000	N	-0.147954	-1.877439	0.000000
O	0.142793	2.233508	0.000000	O	0.141823	2.227635	0.000000
H	-0.723126	2.655532	0.000000	H	-0.722521	2.649234	0.000000
H	-2.170732	0.803277	0.000000	H	-2.166927	0.805103	0.000000

(U)B3LYP/cc-pVTZ				(U)M06-2X/cc-pVTZ			
3β				3β			
C	-1.059891	-1.179741	0.000000	C	-1.055052	-1.179676	0.000000
C	-1.176010	0.202910	0.000000	C	-1.169012	0.201812	0.000000
C	0.000000	0.958114	0.000000	C	0.000000	0.958195	0.000000
C	1.173932	0.237252	0.000000	C	1.174194	0.241491	0.000000
C	1.233123	-1.129423	0.000000	C	1.222647	-1.125593	0.000000
H	-1.955020	-1.791167	0.000000	H	-1.952288	-1.787069	0.000000
H	-2.138973	0.696284	0.000000	H	-2.130910	0.695503	0.000000
H	2.165340	-1.679234	0.000000	H	2.158732	-1.669501	0.000000
N	0.095046	-1.845368	0.000000	N	0.095990	-1.847723	0.000000
O	-0.072990	2.310481	0.000000	O	-0.074843	2.305565	0.000000
H	0.820330	2.673180	0.000000	H	0.814617	2.673236	0.000000

Computed IR Spectra:

In order to analyze the experimental vibrational spectra, theoretical IR spectra have been calculated for photochemical products at (U)B3LYP/cc-pVTZ level of theory.





Curriculum vitae

Academic Qualifications

- 08/2014-Present** **Integrated BS-MS (chemistry majors)**
Department of Chemical Sciences
IISER Mohali, Punjab
Cumulative performance index(CPI)- **7.5/10** (up till 9/10 semesters)
- 04/ 2013 – 03/2014** **12th (Senior Secondary Examination)**
Central Board of Secondary Education
Jaipur, India
Academic performance- **84.0%**
- 04/2011- 03/2012** **10th (Secondary Examinations)**
Central Board of Secondary Education
Jaipur, India
Academic Performance- **CGPA 8.6/10**

Research Experience

05/2018 – 05/2019 **Final year Thesis**

Guide - Dr. Sugumar Venkataramani

Title - *Computational Studies of pyridyl oxy and hydroxy pyridyl radicals.*

05/2017 – 07/2017 **Summer Internship**

Guide - Dr. Sugumar Venkataramani

Title - *Electronic Structure of pyridyl oxy and hydroxy pyridyl radicals.*

05/2016 – 07/2016 **Summer Internship**

Guide - Prof. K.V.R. Chary

Title - *Understanding the Nature of Intrinsically Disordered Protein*

05/2015 – 07/2015 **Summer Internship**

Guide - Prof. Narayanasami Sathyamurthy

Title - *Theory Of Optical Activity*

Conferences

- Presented a poster in *Recent advances in organic and bio-organic chemistry (ROABC, March 2019)* at IISER Mohali

Teaching Experience

- Teaching Assistant for the lab course CHM211 of BS-MS dual Degree programme titled 'Spectroscopic and Other Physical Methods.' **Aug –Dec 2018**
- Teaching Assistant for the lab course CHM212 of BS-MS dual Degree programme titled 'Purification and Separation Technique Lab.' **Jan-April 2019**

Achievements

- INSPIRE Scholar (Funded by Department of Science and Technology, India), 2014-19